Saudi Pharmaceutical Journal 29 (2021) 1466–1485

Contents lists available at ScienceDirect

Saudi Pharmaceutical Journal

journal homepage: www.sciencedirect.com

Original article

Intranasal delivery of Clozapine using nanoemulsion-based *in-situ* gels: An approach for bioavailability enhancement

Nourhan A. Abdulla [a,*], Gehan F. Balata [a,b], Hanaa A. El-ghamry [a], Eman Gomaa [a]

[a] Department of Pharmaceutics, Faculty of Pharmacy, Zagazig University, Zagazig, Egypt
[b] Department of Pharmacy Practice, Faculty of Pharmacy, Heliopolis University, Cairo, Egypt

ARTICLE INFO

Article history:
Received 21 September 2021
Accepted 10 November 2021
Available online 15 November 2021

Keywords:
Pseudoternary phase diagram
Transcutol P
Emulsification time
Pluronic® gel
Ex-vivo permeation
Nasal ciliotoxicity

ABSTRACT

Limited solubility and hepatic first-pass metabolism are the main causes of low bioavailability of anti-schizophrenic drug, Clozapine (CZP). The objective of the study was to develop and validate nanoemulsion (NE) based *in-situ* gel of CZP for intranasal administration as an approach for bioavailability enhancement. Solubility of CZP was initially investigated in different oils, surfactants and co-surfactants, then pseudoternary phase diagrams were constructed to select the optimized ratio of oil, surfactant and co-surfactant. Clear and transparent NE formulations were characterized in terms of droplet size, viscosity, solubilization capacity, transmission electron microscopy, *in-vitro* drug release and compatibility studies. Selected NEs were incorporated into different *in-situ* gel bases using combination of two thermosensitive polymers; Pluronic® F-127 (PF127) and F-68 (PF68). NE-based gels (NG) were investigated for gelation temperature, viscosity, gel strength, spreadability and stability. Moreover, selected NGs were evaluated for *ex-vivo* permeation, mucoadhesive strength and nasal ciliotoxicity. Peppermint oil, tween 80 and transcutol P were chosen for NE preparation owing to their maximum CZP solubilization. Clear NE points extrapolated from tween 80:transcutol P (1:1) phase diagram and passed dispersibility and stability tests, demonstrated globule size of 67.99 to 354.96 nm and zeta potential of −12.4 to −3.11 mV with enhanced *in-vitro* CZP release (>90% in some formulations). After incorporation of the selected N3 and N9 formulations of oil:Smix of 1:7 and 2:7, respectively to a mixture of PF127 and PF68 (20:2% w/w), the resultant NG formulations exhibited optimum gelation temperature and viscosity with enhanced CZP permeation and retention through sheep nasal mucosa. Ciliotoxicity examinations of the optimum NGs displayed no inflammation or damage of the lining epithelium and the underlying cells of the nasal mucosa. In conclusion, NE-based gels may be a promising dosage form of CZP for schizophrenia treatment.

1. Introduction

Clozapine (CZP) is the gold standard in treatment of schizophrenia, severe chronic brain disorder (Opare-Addo et al., 2020). It is a tricyclic dibenzodiazepine and classified as an atypical antipsychotic agent. It is available as oral tablets and suspensions (Food and Drug Administration, 2021). CZP, as a serotonin (5-HT) antagonist, has a unique pharmacological profile via its strong affinity to 5-$HT_{2A/2C}$ receptors and weak antagonistic action on dopamine (D_2) receptor (Stępnicki et al., 2018). CZP is proved to be more effective in treating both positive and negative symptoms in severely-ill schizophrenic patients who are refractory or intolerant to standard antipsychotics (Grinchii and Dermenvoc, 2020; Novakovic and Sher, 2012). The common adverse effects experienced by oral administration of Clozapine include: gastrointestinal effects (hypersalivation, nausea and constipation), metabolic effects (hyperglycaemia, hyperlipidaemia and weight gain), cardiac effects (orthostatic hypotension, myocarditis and tachycardia) and haematological effects (neutropenia and agranulocytosis) (Martindale, 2014).

According to the Biopharmaceutical Classification System, CZP is a class II drug of high permeability and low solubility. It is rapidly and completely absorbed after oral administration meanwhile possessing extensive first-pass metabolism with subsequent

* Corresponding author.
E-mail addresses: nourhan.adel.moh94@gmail.com (N.A. Abdulla), gf_balata@yahoo.com (G.F. Balata), hanaaelghamry@yahoo.com (H.A. El-ghamry), eman_pharmaceutics@yahoo.com (E. Gomaa).
Peer review under responsibility of King Saud University.

Production and hosting by Elsevier

https://doi.org/10.1016/j.jsps.2021.11.006
1319-0164/

low bioavailability (>27%) (Manjunath and Venkateswarlu, 2005; Velupula and Janapareddi, 2019). Additionally, non-compliance to therapy and refraining of schizophrenic patients from swallowing oral medicines, as reported for 50% of patients, may result in poor therapeutic outcomes (Chaudhari et al., 2017). Recently, many formulations of CZP were developed to improve compliance and control agitation in patients with schizophrenia including nanoparticles for injectable delivery (Panda et al., 2016), proniosomes for transdermal delivery (Tareen et al., 2020), etc. However, these formulations suffer from some demerits including particles aggregation or sedimentation, limited drug loading and leakage on storage (Jeevanandam et al., 2018; Sankar et al., 2010). Additionally, previous literature reported the successful administration of CZP via the intranasal route using different systems. Velupula and Janapareddi (2019) formulated CZP as intranasal thermosensitive mucoadhesive *in-situ* gels with improvement in *ex-vivo* flux rate. Tan et al. (2020) prepared CZP-loaded PLGA nanoparticles using supercritical fluid to avoid the use of organic solvents. Patel et al. (2021a) designed CZP as an intranasal nanosuspension using (+)-alpha-tocopherol polyethylene glycol 1000 succinate for enhancing the poor pharmacokinetic parameters of CZP. Patel et al. (2021b) formulated CZP-loaded nanostructured lipid carriers as nose to brain delivery system. In addition, Sayed et al. (2021) used Technetium-99 m radio labeled mixed micelles to investigate the efficiency of CZP targeting to brain.

The intranasal route is emerged as an alternative route to the oral administration as well as for bioavailability enhancement (Adnet et al., 2020; Bayanati et al., 2021; Omar et al., 2019). It avoids first-pass metabolism and provides higher drug absorption due to the porous nature of endothelial membrane of nasal mucosa with high blood supply and large surface area (Vibha, 2014). Moreover, it crosses the blood brain barrier and obviates the need for systemic administration and its potential adverse effects (Adnet et al., 2020).

Nanoemulsion (NE) systems are metastable submicron dispersions of two or more immiscible liquids (aqueous and oily phases). One of these liquids is dispersed uniformly throughout the other by the aid of a mixture of surfactants and cosurfactants forming small droplets in the nanometer range of 10–300 nm (Kreilgaard et al., 2000; Sheth et al., 2020; Song et al., 2021). NEs possess many advantages including dose reduction by improving the solubility and dissolution of hydrophobic drugs, rapid drug action and ease of manufacture and scaling up. They improve the performance of bioactive compounds through triggered and targeted drug delivery (Baghel et al., 2020). In addition, NEs are considered the premium for nasal delivery as they do not require chemical enhancers to facilitate drug transportation through the nasal mucosa and they are more stable than other vesicular systems such as liposomes, ethosomes and niosomes (Bonferoni et al., 2019; Chime et al., 2014). Nevertheless, the direct nasal administration of NEs is inconvenient because of the low viscosity of the system followed by its rapid leakage from the nose. Hence, it is noteworthy to incorporate the CZP-loaded NEs into hydrogel system (NG).

In-situ gel systems are referred to polymer solutions that can be administered as liquids and then undergo a phase transition to semisolid gels upon exposure to physiological environments (Ibrahim et al., 2021). Various mechanisms can lead to formation of *in-situ* gels such as alteration of pH, ionic cross-linkage and variation of temperature (Jagdale et al., 2016). Their fluid-like consistency prior to contact with nasal mucosa can allow their easy instillation and accurate drug dosing (Jaiswal et al., 2012). In addition, their long retention time at the application site can increase drug permeation through the nasal mucosa with subsequent bioavailability enhancement (Patel et al., 2014). The most commonly used thermosensitive *in-situ* gels are those prepared from triblock poly(ethyleneoxide)-poly(propyleneoxide)-poly(ethylene oxide) polymers popularly known as Pluronics®. These gelling agents possess potential features for their usage as intranasal delivery vehicles (Aderibigbe, 2018). They have good solubilization capacity for poorly water-soluble drugs where they are incorporated and fully dissolved in the hydrophobic core of the polymer. In addition, they can promote drug absorption and permeation across the nasal mucosa by disturbing the lipid membranes and decreasing the viscosity of the mucus. Such polymers are non-toxic, non-irritant and provide sustained release of drugs by increasing residence time and viscosity of the preparation (Wang et al., 2013, Zhao et al., 2014).

Since non-compliance to oral dosing of antipsychotics constitutes a major problem towards patients' comfort and effectiveness of therapy, development of a new dosage form of CZP may properly improve the management of schizophrenia (Patel et al., 2021a). Accordingly, the aim of the work was to formulate and validate different CZP-loaded NE gels for intranasal route with an attempt to improve drug bioavailability, reduce systemic adverse effects and improve patient compliance.

2. Materials and methods

2.1. Materials

CZP was kindly supplied by Delta Pharm Co., Egypt. Labrafil isostearique, labrafil M 1944 CS, plurol oleique CC 497, peceol TM, lauroglycol 90, transcutol P and labrafac PG were kindly provided by Gattefossé Co., France. Isopropyl palmitate (IPP), oleic acid, Pluronic® F-127 (PF127) were purchased from Sigma Aldrich Co., USA. Glycerin, paraffin oil, tween 20, tween 80, propylene glycol (PG), polyethylene glycol 400 (PEG 400), ethanol, sudan III and methylene blue were purchased from El-Nasr Pharmaceutical Chemicals Co., Egypt. Eucalyptus oil was purchased from Katto Flavors and Fragrance co., Egypt. Triacetin was purchased from Euromedex Co., France. Pluronic® F-68 (PF68) was purchased from Caisson Laboratories, USA. Peppermint oil was purchased from V. Mane Fils Co., France. Other chemicals and solvents were of analytical grade.

2.2. Methods

2.2.1. Screening the components of NE

Screening of NE components was based on the determination of CZP solubility. Excess amount of CZP was dispersed in 5 ml of different oils, surfactants and cosurfactants in stoppered glass vials. The vials were equilibrated for 72 h in a thermobalanced shaker water bath adjusted at 25 ± 1 °C. Samples were centrifuged at 10000 rpm for 15 min, filtered through 0.45 μm syringe filter membranes. The amounts of CZP in the filtrates were determined spectrophotometrically using UltraViolet–Visible (UV–Vis) spectrophotometer after appropriate dilution with absolute ethanol at 236 nm using the corresponding media as blank (Atodaria and Mashru, 2018). The investegated oils were peppermint oil, triacetin, oleic acid, eucalyptus oil, labrafac PG, peceol TM, IPP and paraffin oil. Tween 80, tween 20, labrafil M 1944 CS and labrafil isostearique were tested as surfactants, while transcutol P, PEG 400, lauroglycol 90, plurol oleique CC 497, ethanol, PG and glycerin were the tested cosurfactants.

2.2.2. Validation of surfactant selection

The four tested surfactants were screened for their miscibility with the highest amounts of oil. Briefly, a fixed volume (4 μl) of the selected oil having the highest solubilization capacity of CZP was added to each aqueous surfactant solution (2.5 ml of 15% w/

w) under high vortexing. The addition of oil was repeated until the clear solution became cloudy (Azeem et al., 2009).

2.2.3. Validation of cosurfactant selection

At a fixed surfactant:cosurfactant (Smix) ratio of 1:1, pseudoternary phase diagrams were constructed using different cosurfactants in order to validate the composition of NE. Each point inside these diagrams were formulated and examined visually for clear one-phase solution formation. Comparing the area of clear NE regions inside phase diagrams was the assessment criterion for selection of a cosurfactant (Azeem et al., 2009).

2.2.4. Pseudoternary phase diagrams construction

Pseudoternary phase diagrams were constructed for the three components of NE (oil, Smix and water) to obtain the concentration ranges revealing the large existence of NE regions at room temperature (Shah et al., 2019). First, the selected surfactant and cosurfactant were mixed at fixed weight ratios (1:0, 1:1, 1:2, 1:3, 2:1 and 3:1, respectively) to prepare the Smix. The selected oil was then incorporated into the prepared Smix at different proportions. Finally, water was added gradually under vortexing until a transparent and easy flowable NE was obtained. The resulted pseudoternary phase diagrams were investigated to select the ratio of Smix showing the largest NE region for further characterization.

2.2.5. Preparation of CZP-loaded NEs

At room temperature, the appropriate amounts of Smix and oil were mixed together, vortexed till complete dispersion and then CZP was added at a ratio of 2.5% w/w (equivalent to 25 mg). The final mixtures were vortexed for 10 min until transparent NEs were obtained.

2.2.6. Characterization of CZP-loaded NEs

2.2.6.1. Determination of emulsion type. The emulsion type either oil in water (o/w) or water in oil (w/o) was determined by dye test using either water soluble (methylene blue) or oil soluble (sudan III) dye. Based on the dispersibility of water soluble dye in the aqueous phase and oil soluble dye in the oil phase, these dyes were added to the formulated NEs and examined under optical microscope in order to determine the type of emulsion (Roohinejad et al., 2015).

2.2.6.2. Dispersibility, self-nanoemulsification time and % transmittance measurements. The dispersibility and self-nanoemulsification time were evaluated by adding 1 ml of each NE to 200 ml of distilled water maintained at 34 °C using a hot plate with magnetic stirring at 50 rpm. The homogeneity of formulations was visually assessed by recording the time needed for incidence of complete nanoemulsification according to the following grades;

- Clear or slight blue emulsion obtained within 1 min (classified as grade A)
- Less clear or bluish white emulsion obtained within 1 min (classified as grade B)
- Milky white emulsion obtained within 2 min (classified as grade C)
- Dull and greyish white emulsion obtained after 2 min having oily appearance and slower emulsification (classified as grade D)
- Formulation having large oil globules on the surface and poor emulsification (classified as grade E).

Moreover, % transmittance of formulations was determined with UV–Vis spectrophotometer using distilled water (blank). The nano-size of formulations could be manifested by % transmittance values close to 100% (Gaba et al., 2019). Formulations that passed the dispersibility tests in grades A and B and had % transmittance values close to 100% were subjected for the subsequent studies (Balata et al., 2016).

2.2.6.3. Thermodynamic stability studies. The thermodynamic stability of the prepared formulations was determined through three-steps procedure. At the beginning, samples were centrifuged at 15000 rpm for 30 min and those showed any sign of phase separation, creaming or cracking were discarded. Then, samples were stored under six successive cycles of heating (45 °C) and cooling (4 °C) for not<48 h at each temperature to determine the consequence of temperature variations on their stability. Finally, three freeze–thaw cycles were done for the formulations between −20 and 25 °C with storage at each temperature for 48 h to observe their efficient dispersibility. Formulations only survived after these tests were selected for further studies (Azeem et al., 2009; Chintalapudi et al., 2015).

2.2.6.4. Determination of globule size, poly dispersibility index (PDI) and zeta potential of NEs. The samples were subjected to dynamic light scattering technique using Malvern Master-sizer 2000 having built-in Zeta-sizer. Samples were diluted with deionized water (1:100) to avoid multiple scattering effects, added in a polystyrene disposable cuvette and fixed in the direction of laser light beam. The globule size, PDI and zeta potential of the tested formulations were recorded.

2.2.6.5. pH and viscosity measurements. A glass electrode of a digital pH meter was dipped in each tested NE sample (30 ml) for measuring the pH values at 25 °C. In addition, viscosity of different samples was measured using Viscostar-R viscometer with spindle no.6 at 100 rpm.

2.2.6.6. Solubilization capacity measurement. The maximum amount of CZP that can be dissolved in 1 ml NE was determined by adding excess amount of CZP to 5 ml of each NE formulation in stoppered glass vials. The vials were equilibrated for 72 h in a thermobalanced shaker water bath adjusted at 25 ± 1 °C. Samples were centrifuged at 10000 rpm for 15 min and filtered through 0.45 μm syringe filter membranes. The amounts of CZP in the filtrates were quantified after appropriate dilution with absolute ethanol by UV–Vis spectrophotometer at 236 nm using the corresponding media as blank.

2.2.6.7. Drug content measurement. The NE formulations containing CZP equivalent to 25 mg were diluted with absolute ethanol and analyzed for drug content using UV–Vis spectrophotometer (236 nm) against absolute ethanol as a blank. The drug content was determined according to the following equation (Edresi and Baie, 2009):

$$\text{Drug content } (\%) = \frac{\text{Analyzed drug content}}{\text{Theoretical drug content}} \text{ x } 100$$

2.2.6.8. Transmission electron microscopy (TEM). The study of morphology and structure of NE globules was based on the bright imaging technique with high magnification and diffraction using TEM. The formulated samples were diluted with water (1:10), directly loaded on 200-mesh carbon-coated cupper grid and examined at 200 kV using transmission electron microscope (JEM-2100, JEOL, Japan).

2.2.6.9. In-vitro drug release studies. Dialysis bags were washed with deionized water and soaked overnight in phosphate buffer saline (PBS) of pH 6.4 corresponding to the pH of nasal fluid. A vol-

ume of NE equivalent to 25 mg of CZP was placed in a dialysis bag suspended in 200 ml PBS of pH 6.4 as a release medium. The receptor media containing bags were kept in a thermobalanced water bath shaker at 34 ± 0.5 °C similar to the temperature of the nasal cavity and 50 rpm (Altuntaş et al., 2017). 3 ml samples were taken at predetermined time intervals (0, 0.5, 1, 2, 3, 4, 5, 6, 7, 8 and 24 h) and replaced with fresh medium of the same volume to maintain the sink condition. These samples were analyzed by UV–Vis spectrophotometer at 236 nm in comparison to pure drug suspension. The release profiles of CZP-loaded NEs were expressed as cumulative % of drug released plotted versus time.

2.2.6.10. Release kinetic analysis. The *in-vitro* release data of CZP-loaded NEs were analyzed according to various kinetic models:

Zero-order model: $R = K_o t$ (Huo et al., 2021),

First-order model: $R = 1 - e^{-kt}$ (Mohamad et al., 2021),

Higuchi model: $R = K_H\, t^{1/2}$ (Huo et al., 2021),

Hixson-Crawell model: $W_o^{1/3} - W_t^{1/3} = K_{HC}\, t$ (Craciun et al., 2019) and

Korsmeyer-Peppas model: $R = k_{KP}\, t^n$ (Abdul Rasool et al., 2021),

Where R is the amount of drug released at time t; k_o, k, k_H, K_{HC} and k_{Kp} are rate constants for zero-order, first-order, Higuchi, Hixson-Crawell and Korsmeyer-Peppas kinetic models, respectively; n is the release exponent in the Korsmeyer-Peppas model; W_o is the initial amount of drug and W_t is the amount of drug remaining at time t. The model having highest correlation coefficient (R^2) was used for the assessment of CZP release mechanism to best describe its release behavior.

2.2.6.11. Stability (temperature stress) studies. Based on the characterization tests, selected NE formulations were examined for short term stability or temperature stress studies. The tested samples were transferred to sealed glass containers for storage at different temperature conditions; in refrigerator (4 °C) and at ambient temperature (25 °C) over 90 days. They were visually observed for their physical appearance or any sedimentation. Further assessments for % transmittance, pH, viscosity, drug content, globule size, PDI and zeta potential were employed as previously described. All experiments for characterization were carried out in triplicates (n = 3) and the values were expressed as mean ± S.D.

2.2.7. Thermosensitive in-situ gels formulation

2.2.7.1. Preliminary studies for preparation of NE-based gels (NGs). The thermosensitive PF127 polymeric gel was prepared by using cold method. The polymer base at different concentrations of 18–23% w/w was added gradually into the required amount of cold distilled water with continuous stirring for 15 min. The dispersions were refrigerated overnight at 4 °C until clear gels were obtained. The prepared samples were examined for gelation and formation of acceptable gels at the solution-gel temperature (Tsol-gel) range of 30–32 °C (Okur et al., 2020). The selected CZP-loaded NE formulations were then added drop wise individually at various ratios to the formed polymeric gels (1:1, 1:2, 1:3, 1:4 and 1:5 respectively) with gentle stirring by using magnetic stirrer to monitor whether changes in the Tsol-gel could occur. Because of unsatisfactory Tsol-gel results upon incorporation of NE formulations into the PF127 gels at different ratios, combinations of PF127 (20% w/w) with various ratios of PF68 (1–5% w/w) were studied. Optimum NG formulations with acceptable Tsol-gel values were selected for further investigations.

2.2.8. Characterization of CZP-loaded NGs

2.2.8.1. Visual assessment for clarity. The prepared formulations were inspected for clarity, grittiness and color against a white background. Smears of formulations were spread on glass slides and observed for presence of any insoluble particles, aggregates or grittiness.

2.2.8.2. Determination of Tsol-gel and gelation time (GT). The tube inversion method was followed to measure the Tsol-gel of the prepared formulations. In a test tube, exactly 2 g of each prepared formulation was immersed in a thermobalanced water bath and the temperature was elevated gradually from 22 to 37 °C with an increment of 1 °C until the gelation occurred. The temperature remained constant for 5 min at each point and the flow of gels was observed after the immediate inversion of the test tubes and the GT was recorded (Qian et al., 2014). Formulations that passed the Tsol-gel and GT tests were selected for the following studies.

2.2.8.3. pH and viscosity measurements. The pH values of the selected NG formulations were determined by dipping the glass electrode of a digital pH meter into a 50 ml beaker containing a sufficient quantity of each prepared formulation at room temperature. The samples were allowed to equilibrate for 5 min and the viscosity was determined at 25 °C (solution form) and at physiological temperature i.e. 31 °C (gel form) using Viscostar-R viscometer with spindle no.6 at 100 rpm (Zaki et al., 2007).

2.2.8.4. Gel strength measurement. The time in seconds required for a weight of 35 g to move down 5 cm through 50 g gel placed in a 100 ml graduated measuring cylinder was calculated as gel strength (Maheswara et al., 2011).

2.2.8.5. Spreadability measurement. Briefly, 1 g of each NG formulation was placed within a circle of 1 cm diameter drawn on glass plate and covered by another one. Then, a second glass plate was placed over the first one and a specific weight (500 g) was located on the upper plate for 5 min until the spreading of gel formulations stopped. The increment of circle diameter of gels was recorded as the spreadability value (Mbah et al., 2019).

2.2.8.6. In-vitro drug release study. Each sample of the selected NG formulations equivalent to a single dose (25 mg) of CZP was placed in a dialysis bag immersed in 200 ml of PBS (pH 6.4) as a receptor medium. The media were kept in a thermobalanced water bath shaker at 34 ± 1 °C and 50 rpm. 3 ml samples were withdrawn at predetermined time intervals (0, 0.5, 1, 2, 3, 4, 5, 6, 7, 8 and 24 h) and replaced by equal volumes of fresh release medium to maintain the sink condition. The samples were analyzed using UV–Vis spectrophotometer at 236 nm in comparison to control gel formulation containing pure CZP dispersed in PF127 and PF68 mixture (20:2% w/w). The release profile was expressed as cumulative % of CZP released and plotted versus time. All experiments were repeated three times (n = 3) and the results were expressed as mean ± S.D.

2.2.8.7. Differential scanning colorimetry (DSC). The DSC study of pure CZP, selected oil, surfactant, cosurfactant, blank NE and selected CZP-loaded NE and NG formulations was performed using DSC instrument (DSC W70, Shimadzu, Japan). About 2 mg of each sample was weighed, sealed in standard DSC aluminum pan and scanned over a temperature range from 25 to 250 °C at a heating rate of 10 °C/min. The empty aluminum pan was used as reference cell under nitrogen purge (30 ml/min).

2.2.8.8. Fourier transform infrared (FTIR) spectroscopy. Pure CZP, selected oil, surfactant, cosurfactant, blank NE and selected CZP-loaded NE and NG formulations were scanned using Perkin-Elmer FTIR spectrophotometer (series 1600, Perkin-Elmer Corporation, USA) under vacuum from 4000 to 500 cm^{-1} through potassium bromide disk method.

2.2.8.9. Ex-vivo drug permeation study.

2.2.8.9.1. Isolation of sheep nasal mucosa. *Ex-vivo* permeation study was carried out for the optimum CZP-loaded NG formulations using fresh nasal mucosa obtained from sheep head brought from local slaughter house immediately after its sacrifice. A sagittal cut was made at the middle of the head to expose nasal anatomy. The intact nasal mucosa was separated from the septum and connective tissue. The nasal mucosa was kept in PBS (pH 6.4) for 30 min for equilibration, then fixed onto a diffusion cell. Amount of each formulation (equivalent to 25 mg CZP) was placed in the donor compartment of a diffusion cell suspended in a thermobalanced water bath shaker. The temperature of the receiver chamber containing 200 ml PBS (pH 6.4) was kept at 34 ± 1 °C. Samples of 3 ml were withdrawn at successive time intervals (0, 1, 2, 3, 4, 5, 6, 7, 8 and 24 h) and replaced by equal volumes of fresh release medium to maintain the sink condition. The permeation of CZP from NG formulations was monitored in comparison to that of the control gel (Jaiswal et al., 2012; John et al., 2013).

The drug content was detected by high performance liquid chromatography (HPLC) analysis using Waters 2690 Alliance HPLC system equipped with photodiode array detector and column C18 (Scharlau: 4.6 × 250 mm, 5 µm). Exactly 0.5 ml of each sample was added to 0.5 ml of mobile phase consisting of 0.05 M potassium buffer and acetonitrile (65:35%). Then, 3 ml triethylamine was added and the pH was adjusted to 4.5 with orthophosphoric acid. Samples were filtered using 0.22 µm nylon syringe filters then 100 µl were injected at ambient temperature with flow rate of 1 ml/min and wavelength of 257 nm.

2.2.8.9.2. Permeation data analysis. The cumulative amount of drug permeated through the nasal mucosa (µg/cm^2) was plotted versus time (t) for each formulation (Baboota et al., 2007). Permeation analysis was performed according to the following equations:

$$Jss = \frac{\text{Slope of linear portion of graph}}{\text{Area of diffusion cell}}$$

Where, Jss is the drug flux (permeation rate) at steady state.

$$K_p = \frac{Jss}{C_o}$$

Where, Kp is the permeability coefficient and C_o is the initial concentration of drug in the donor cell.

$$Er = \frac{Jss\ of\ formulation}{Jss\ of\ control}$$

where, Er is the enhancement ratio of the tested formulation to the control formulation.

2.2.8.9.3. Mucosal deposition study. The mucosal deposition study of the tested CZP-loaded NG formulations were carried out to determine the content of CZP deposited in the nasal mucosa after 24 h of drug permeation. At the end of *ex-vivo* permeation study, the mucosal membranes were cleaned using a cotton swab soaked with ethanol for several times to clear their surfaces from excess CZP. The membranes were cut into different pieces, placed into 10 ml ethanol for drug extraction, vortexed for 5 min and then centrifuged at 6000 rpm for 30 min. The supernatants were filtered using syringe filter membranes and their drug contents were quantified spectrophotometrically at 236 nm using the corresponding medium as a blank (Sarwal et al., 2019). The measurements were compared with that of the control gel formulation.

2.2.8.10. Mucoadhesive strength study. Mucoadhesive potential of the tested NG formulations was measured using modified physical balance and fresh sheep nasal mucosa as the biological membrane. The method was based on recording the magnitude of force required to detach the formulation from the nasal membrane. The right pan of balance was replaced with an empty plastic cup. The left pan was replaced with two attached glass vials (base to base). The base of each vial was attached with fresh nasal mucosa moistened with PBS of pH 6.4. The tested NG formulations equivalent to 25 mg of CZP were placed on the lower vial then the vials were held together. A specific weight was placed on the upper vial for 2 min to expel the entrapped air between both vials and assure the intimate contact. The weight was removed and water was added slowly at a constant rate to the plastic cup until both vials were detached (Chaudhary and Verma, 2014). The mucoadhesive strength in dyne/cm^2 was determined by using the following formula:

Mucoadhesive strength = $\frac{m \times g}{A}$ where, m is the weight of the added water (g), g is the acceleration due to gravity (980 cm/s^2) and A is the area of the exposed mucosa (cm^2). The measurements were compared to that of the control gel formulation.

2.2.8.11. Nasal ciliotoxicity study. Four fresh sheep nasal mucosal pieces with uniform thickness were investigated. The first piece (negative control) was treated with 0.5 ml saline. The second piece was treated with 0.5 ml of strong mucociliary toxin (isopropyl alcohol) and utilized as a positive control. The third and fourth pieces were treated with the selected NG formulations. After 1 h, the mucosal membranes were rinsed with PBS (pH 6.4) and kept overnight in 10% neutral Formalin. Then, they were cut vertically and dehydrated with a graded series of ethanol. These pieces of mucosa were embedded in paraffin blocks and fine sections were taken with the microtome and stained with hematoxylin and eosin. The sections were examined under microscope (polarizing microscope RPL-55 series, Radical Instruments, India) and photographed using Nikon optiphot (magnification × 400) (Gaba et al., 2019; Patel et al., 2016).

2.2.8.12. Stability studies. The selected NG formulations were evaluated for short term stability study. The samples were transferred to sealed glass containers for storage at room temperature and at 4 °C. Samples were visually inspected for their physical appearance after 30, 60 and 90 days and further assessed for Tsol-gel, pH, viscosity, gel strength and spreadability as previously described.

2.2.8.13. Statistical analysis. One-way analysis of variance (ANOVA) was used to evaluate the significance of difference ($p < 0.05$) using (GraphPad PrismVR program, version 5.00).

3. Results and discussion

3.1. Screening the components of NE

Screening of NE components was determined by evaluation of CZP solubility in different oils, surfactants and cosurfactants (Table 1). Peppermint oil showed the premier record in solubilizing CZP (201.95 ± 3.14 mg/ml), since, it was the oil of choice.

The dual nature of surfactants gives them a vital role in formulating and stabilizing NEs by being able to bridge the gap between the immiscible water and oil phases and thus reduce the interfacial tension with minimization of the energy required for NE formation (Sulaimon and Adeyemi, 2018). Moreover, surfactants can interfere with coalescence of globules by forming stearic barrier in addition to interfering with the lipid bilayer and consequently improving permeability into the epithelial membrane (Patel et al., 2016). Tween 80, as a non-ionic surfactant of hydrophilic-lipophilic balance (HLB) value of 15, provided a maximum solubilizing capacity for CZP (76.01 ± 3.48 mg/ml). Moreover, tween 80 was capable of formation of o/w NE with fine and uniform globules and then was selected for NE formulation (Pavoni et al., 2020). In addition,

Table 1
Solubility measurements of CZP in different oils, surfactants and cosurfactants.

Oils	Solubility (mg/ml)	Surfactants	Solubility (mg/ml)	Cosurfactants	Solubility (mg/ml)
Peppermint oil	201.95 ± 3.14	Tween 80	76.01 ± 3.48	Transcutol P	60.26 ± 2.10
Triacetin	144.13 ± 1.16	Tween 20	35.23 ± 3.32	PEG 400	38.31 ± 0.81
Oleic acid	111.5 ± 1.74	Labrafil M 1944 CS	26.93 ± 1.13	Lauroglycol 90	38.14 ± 2.94
Eucalyptus oil	99.53 ± 2.84	Labrafil isostearique	23.96 ± 1.50	Plurol oleique CC 497	36.26 ± 3.16
Labrafac PG	41.38 ± 0.11	–	–	Ethanol	34.75 ± 2.21
Peceol TM	28.11 ± 2.66	–	–	PG	27.57 ± 1.17
IPP	16.32 ± 1.78	–	–	Glycerin	14.09 ± 0.24
Paraffin oil	6.21 ± 0.71	–	–	–	–

IPP, isopropyl palmitate; PEG, polyethylene glycol; PG, propylene glycol.

lower critical micelle concentration and higher *in-vivo* stability profiles of uncharged tween 80 made it the surfactant of choice having low irritant effect with nominal variation in pH (Khani et al., 2015).

Incorporation of a cosurfactant reduces the amount of surfactant used. The cosurfactant can reduce the bending stress by making the interfacial film flexible enough to deform readily around each globule (Gaba et al., 2019; Patel et al., 2016). Moreover, cosurfactants increase the film fluidity and hence its curvature with subsequent formation of NEs over a wide range of composition. Cosurfactants increase the hydrocarbon tail mobility and consequently provide greater penetration of oil in the NE region (Elbardisy et al., 2019). Based on the results of solubility measurements, transcutol P was selected for NE formulation (Table 1). It acts as an efficient permeation enhancer with HLB value of 4.2 (Mura et al., 2011).

3.2. Validation of surfactant and cosurfactant selection

Azeem and co-workers (2009) reported that determination of drug solubility in different surfactants and cosurfactants could not be used solely for identification of NE components. Accordingly, investigation of the miscibility of different surfactants in peppermint oil was employed. Tween 80 showed the highest miscibility with higher volumes of peppermint oil (16 μl; 4 additions of 4 μl of oil) without turbidity or phase separation, while tween 20 showed lower miscibility using only 2 additions of oil (8 μl). It was reported that the solubilty of the oil decreased as the difference between the HLB of oil and surfactant increased. Therefore, tween 80 with HLB value of 15 could solubilize peppermint oil (HLB = 12.3) more than tween 20 with HLB value of 16.7 (Edris and Abd El-Galeel, 2010). Tween series differ in terms of oil solubilization and the emulsification capacity can be explained on the basis of structure of the alkyl chain group (Syed and Peh, 2014). Tween series are structurally similar in the head group of polyoxyethylene, but differs in the tail group. Tween 20 has a medium-chain carbon tail (C12) of saturated lauric acid. While, tween 80 has a long-chained tail group (C18) of unsaturated oleic acid (Mahdi et al., 2011). The presence of the double bond (fluidizing group) in the side chain of tween 80 plays an essential role in oil uptake by decreasing the hydrophicity and enhancing the emulsification process (Aggarwal et al., 2013). On the other hand, labrafil M 1944 CS and labrafil isostearique were immiscible with peppermint oil and turned milky with the first addition of 4 μl of oil.

Regarding the validation of cosurfactants, transcutol P in combination with tween 80 and peppermint oil showed the highest area of clear NEs (area = 48%) in comparison to other tested cosurfactants (Fig. 1). Alternatively, PEG 400 and glycerin exhibited unclear NE regions (area = 0%). Therefore, tween 80 and transcutol P were selected as optimal surfactant and cosurfactant, respectively, for the formation of peppermint oil-based NE owing to their highest capability for solubilizing CZP and being highly miscible with peppermint oil over wide concentration ranges.

3.3. Pseudoternary phase diagrams construction

The phase diagram demonstrates the relationship between the physical appearance of NE and its composition. It was observed that the Smix ratio had great impact on solubilizing the oily phase along with reduction in the free energy of the system (Baboota et al., 2007; Gaba et al., 2019). The diagrams were constructed using peppermint oil, tween 80 and transcutol P without addition of the drug to identify the precise concentration ratio of the components. The shaded areas (Fig. 2) represented the transparent and easily flowable NE regions, whereas the non-shaded areas displayed the milky/multiphase emulsion regions based on careful visual observation (Arora et al., 2014).

At the Smix weight ratio (1:0) (Fig. 2a), it was observed that the least area of the NE region was produced (24%). When transcutol P was equally mixed with tween 80 at 1:1 (Fig. 2b), the NE region was increased by two folds (48%). This was attributed to the fact that addition of transcutol P might lead to greater penetration of the oil phase in the hydrophobic region of the surfactant monomers decreasing the interfacial tension and consequently increasing the interface fluidity and entropy of system (Akhtar et al., 2016). Increasing transcutol P ratio to 1:2 and 1:3 w/w resulted in significant reduction in the area of NE to 40% and 32%, respectively (Fig. 2c and 2d). This was attributed to the low tween 80 concentration that would decrease the amount of micelle leading to minimal solubilization capacity of NE (Tung et al., 2018).

Nevertheless, increasing tween 80 ratio to 2:1 and 3:1 w/w resulted in non-significant reduction in the area of NE (45% and 43%, respectively) (Fig. 2e and 2f). This might be attributed to the fact that increasing the surfactant concentration resulted in more stable NE and produced smaller globule size by its interfacial activity (Shafiq et al., 2007). However, further increase in surfactant concentration might result in production of smaller droplets with more Brownian motion and initiation of Ostwald ripening (Bhattacharjee, 2019). In addition, interfacial disruption might occur as a result of water penetration into the oil droplets and hence ejection of oil droplets into the aqueous phases (Khani et al., 2015). Based on the results of pseudoternary phase diagrams, it could be concluded that the free energy of NE formation was dependent on the extent to which the Smix ratio could minimize the surface tension of the o/w interface thereby influencing the dispersion entropy. Thus, a negative free energy of formulation and satisfactory entropic changes were attained owing to the high decrement of surface tension and increment of interfacial area resulting in spontaneous formation of thermodynamically stable NE (Akhtar et al., 2016; Bhattacharjee, 2019). Therefore, 32 NE points inside the pseudoternary phase diagram of Smix (1:1) were selected for further characterization.

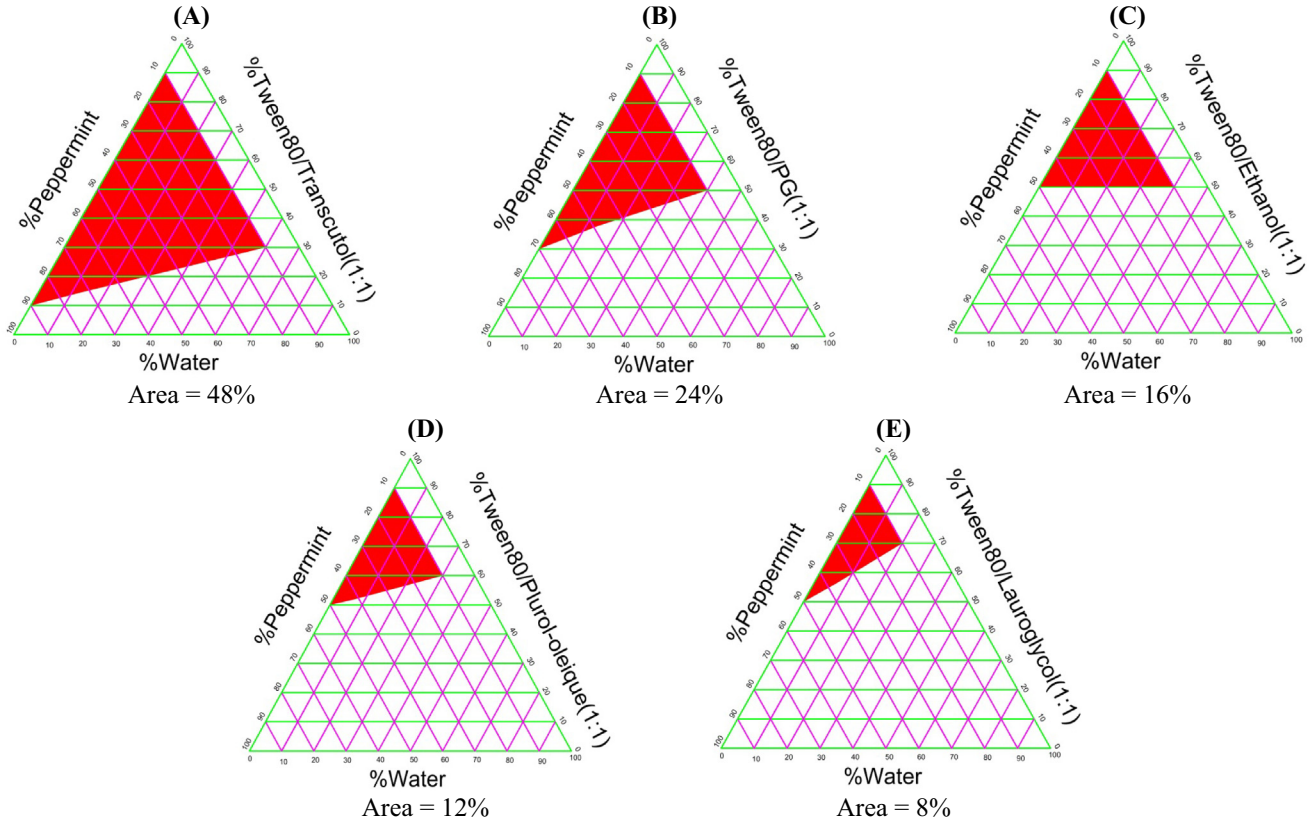

Fig. 1. Study of pseudoternary phase diagrams using different cosurfactants (A) transcutol P (B) PG (C) ethanol (D) plurol oleique CC 497 (E) lauroglycol 90.

3.4. Characterization of CZP-loaded NEs

3.4.1. Determination of emulsion type

The formed NEs were light yellow, clear, transparent and homogeneous without any visible particulates. Regarding the dispersion of methylene blue, it was miscible with different NE formulations and dispersed evenly with no precipitations or clusters indicating that the external phase was hydrophilic and the type NE was o/w (Roohinejad et al., 2015).

3.4.2. Dispersibility, self-nanoemulsification time and % transmittance measurement

Generally, dispersibility test is a valuable index for evaluation of NE efficiency. The tested formulations dispersed completely and rapidly owing to the high solubilizing capacity of the components and their capability to form relatively stable emulsions with nanoscale droplets at infinite water dilution under mild agitation (Chintalapudi et al., 2015). Table 2 shows that the nanoemulsification time increased by increasing the proportion of peppermint oil in the formulation or decreasing the concentration of the Smix. This might be due to the efficiency of Smix to lower the interfacial tension at o/w interface and thus facilitating the dispersion formulation with rapid emulsification rate (Balata et al., 2016).

Furthermore, the % transmittance values of selected NEs were close to that of distilled water (blank) ensuring that oil droplets were small and uniformly distributed throughout the dispersion phase (Gaba et al., 2019). Table 2 demonstrates that % transmittance values of N1-N15 formulations were between 97.74 ± 1.53 and 100.31 ± 0.25%, confirming their optically clear and transparent nature (Patel et al., 2016).

From the oil:Smix ratios examined, only formulations (N1-N15) were graded as A and B and possessed high % transmittance values close to 100%. Therefore, they were selected for further investigation as they resulted in stable NEs upon dilution.

3.4.3. Thermodynamic stability studies

Conventional emulsions have kinetic stability with subsequent separation during storage. While, NE formulations possess thermodynamic stability and this is ascribed not only to the favorable adsorption of surfactant and cosurfactant existing at the o/w interface, but also the avoided coalescence due to reduction of interfacial energy (Azeem et al., 2009; Balata et al., 2016). In order to exclude the possibility of metastable formulations, stress testing was performed for the selected formulations (N1-N15). The results revealed that all formulations passed the test without CZP precipitation, phase separation, creaming or even cracking, which justified the stability of the prepared NEs (Table 2).

3.4.4. Determination of globule size, PDI and zeta potential of NEs

Globule size and PDI are the key factors for prediction of physical stability of the formulation as well as the rate and extent of drug release and absorption (Balata et al., 2016; Elbardisy et al., 2019). It was clear that the oil concentration had significant effect on globule size which was in agreement with Shafiq et al. (2007). Per our results, this was obvious by comparing the mean globule size of N4, N10 and N14 formulations (Table 3). By increasing the concentration of oil (10–30%), the globule size was increased to 77.34 ± 8.83, 94.46 ± 3.44 and 125.53 ± 1.78 nm, respectively. In addition, decreasing the Smix ratio resulted in an increase of the globule size as shown in Table 3. The small globule size can be related to the molecular geometry of the surfactant. Tween 80 has optimum curvatures and packing parameters that can facilitate smaller micelles formation. Due to the unsaturated hydrophobic segments of tween 80, more tangled packing of surfactant can be

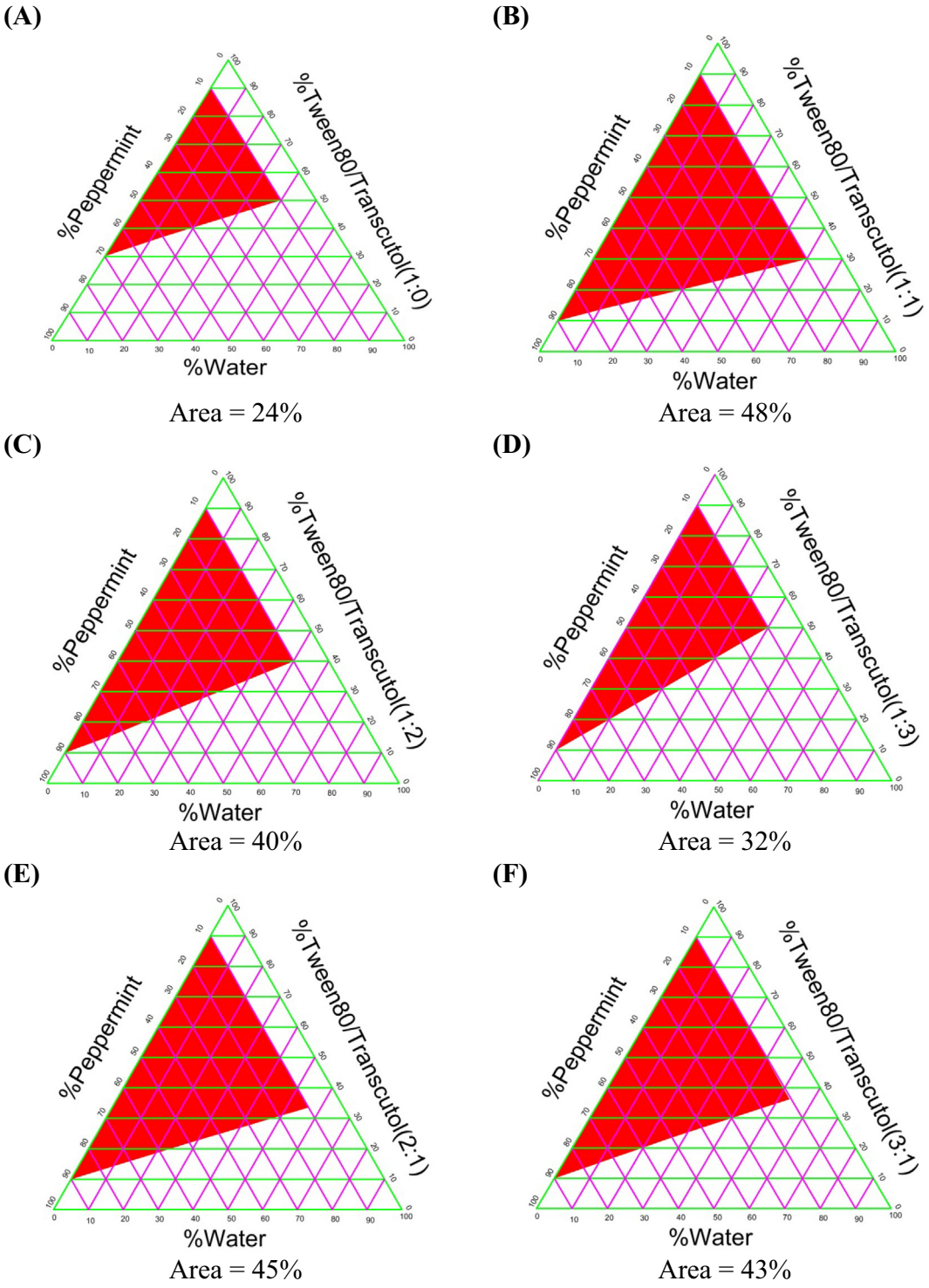

Fig. 2. Study of pseudoternary phase diagrams using peppermint oil, tween 80 and transcutol P at different Smix ratios of (A) 1:0 (B) 1:1 (C) 1:2 (D) 1:3 (E) 2:1 (F) 3:1.

achieved at o/w interface with spontaneous production of fine micelles after mixing the organic and aqueous phases (Abdul Aziz et al., 2019).

PDI indicates the uniformity of globule size of the prepared formulation. The higher the PDI value (0.5–1), the lower the uniformity of the globule size in the NE formulation (Baboota et al., 2007; Elbardisy et al., 2019). As shown in Table 3, low PDI values (0.11–0.34) were obtained which indicated the uniformity of globule size within each formulation.

Zeta potential is a useful parameter to predict the long-term stability of NEs. It represents the electrokinetic potential of ions strongly attached to the surface with a significant difference in viscoelasticity in comparison to the solution adjacent to the particles (Schreiner et al., 2020). It is strongly affected by multiple factors such as surfactants type, ionic strength, morphology, particle size, solution pH and hydration (He et al., 2011). Generally, the stability of NEs can be explained by two theories namely; electrostatic and steric mechanisms. Electrostatic stability is exhibited due to the

Table 2
Characterization of NE formulations in terms of dispersibility grade, color, emulsification time, % transmittance and thermodynamic stability.

Formula	Oil:Smix ratio	Dispersibility grade	Color	Emulsification time (s)	% Transmittance	Thermodynamic stability
N1	1:9	A	Clear	10.67 ± 2.52	99.80 ± 1.16	Pass
N2	1:8	A	Clear	12.33 ± 1.53	100.10 ± 0.15	Pass
N3	1:7	A	Clear	17.33 ± 2.08	99.98 ± 0.10	Pass
N4	1:6	A	Clear	25.00 ± 1.00	100.31 ± 0.25	Pass
N5	1:5	A	Clear	25.33 ± 1.53	99.85 ± 2.40	Pass
N6	1:4	A	Clear	27.33 ± 0.58	99.37 ± 0.47	Pass
N7	1:3	A	Clear	32.67 ± 0.58	99.47 ± 1.15	Pass
N8	2:8	B	Bluish white	34.33 ± 0.58	99.98 ± 1.55	Pass
N9	2:7	A	Clear	40.33 ± 1.53	98.93 ± 0.45	Pass
N10	2:6	A	Clear	33.67 ± 2.52	98.97 ± 0.21	Pass
N11	2:5	A	Clear	35.33 ± 1.53	99.17 ± 2.35	Pass
N12	2:4	B	Bluish white	54.67 ± 0.58	98.33 ± 1.06	Pass
N13	3:7	B	Bluish white	36.00 ± 1.15	97.87 ± 1.35	Pass
N14	3:6	B	Bluish white	37.00 ± 2.00	97.81 ± 0.43	Pass
N15	3:5	B	Bluish white	42.33 ± 0.58	97.74 ± 1.53	Pass
N16	2:3	C	Milky	29.67 ± 1.53	84.37 ± 3.91	NA
N17	3:4	C	Milky	23.67 ± 0.58	64.25 ± 3.71	NA
N18	3:3	C	Milky	32.33 ± 1.53	53.46 ± 1.56	NA
N19	4:6	C	Milky	75.67 ± 3.21	71.63 ± 0.58	NA
N20	4:5	C	Milky	89.33 ± 2.08	56.93 ± 4.32	NA
N21	4:4	C	Milky	27.67 ± 0.58	52.76 ± 1.68	NA
N22	4:3	D	Greyish white	76.67 ± 1.15	63.81 ± 0.69	NA
N23	5:5	D	Greyish white	83.67 ± 2.52	61.62 ± 1.93	NA
N24	5:4	D	Greyish white	87.00 ± 3.00	74.75 ± 0.57	NA
N25	5:3	D	Greyish white	80.33 ± 0.58	73.61 ± 1.78	NA
N26	6:4	C	Milky	93.67 ± 1.15	58.73 ± 2.74	NA
N27	6:3	E	Dull grey, oily layer on the surface	96.33 ± 2.52	63.35 ± 0.89	NA
N28	6:2	E	Dull grey, oily layer on the surface	100.00 ± 1.53	74.93 ± 1.36	NA
N29	7:3	D	Greyish white	65.00 ± 3.00	62.84 ± 1.23	NA
N30	7:2	E	Dull grey, oily layer on the surface	67.33 ± 1.53	72.55 ± 1.48	NA
N31	8:2	E	Dull grey, oily layer on the surface	100.33 ± 2.52	68.67 ± 1.56	NA
N32	9:1	E	Dull grey, oily layer on the surface	70.00 ± 1.00	64.34 ± 3.58	NA

Smix, surfactant:cosurfactant mixture; NA, not applicable.
* All formulations contain water up to 100% w/w.

Table 3
Characterization of NE formulations in terms of globule size, PDI, zeta potential, pH, viscosity, solubilizing capacity and drug content.

Formula	Globule size (nm)	PDI	Zeta potential (mV)	pH	Viscosity (cP)	Solubilizing capacity (mg/ml)	Drug content (%)
N1	79.11 ± 9.56	0.29 ± 0.06	−9.14 ± 2.43	6.43 ± 0.03	23.53 ± 2.03	150.12 ± 1.48	99.16 ± 1.04
N2	67.99 ± 2.43	0.14 ± 0.08	−10.38 ± 1.39	6.46 ± 0.05	12.45 ± 2.70	158.63 ± 1.35	99.95 ± 1.02
N3	73.82 ± 2.43	0.24 ± 0.03	−11.40 ± 0.40	6.43 ± 0.05	18.42 ± 3.80	180.24 ± 2.03	100.03 ± 2.17
N4	77.34 ± 8.83	0.31 ± 0.15	−9.28 ± 1.75	5.83 ± 0.05	21.42 ± 0.88	173.79 ± 1.79	99.64 ± 1.08
N5	84.27± 9.99	0.19 ± 0.02	−7.82 ± 2.03	5.93 ± 0.06	33.64 ± 0.13	69.64 ± 2.31	99.65 ± 1.23
N6	86.47 ± 6.35	0.11 ± 0.006	−7.16 ± 0.92	5.97 ± 0.15	39.34 ± 4.70	59.61 ± 1.43	99.88 ± 1.05
N7	210.00 ± 7.34	0.26 ± 0.06	−3.88 ± 0.70	5.96 ± 0.05	51.64 ± 1.32	43.98 ± 1.74	99.56 ± 1.11
N8	232.33 ± 7.85	0.17 ± 0.03	−4.96 ± 0.47	6.20 ± 0.1	44.73 ± 2.42	246.41 ± 2.16	98.57 ± 2.15
N9	83.40 ± 3.89	0.14 ± 0.03	−12.4 ± 1.73	6.40 ± 0.1	25.84 ± 0.23	265.75 ± 1.54	100.13 ± 2.06
N10	94.46 ± 3.44	0.13 ± 0.04	−8.14 ± 0.98	6.47 ± 0.06	28.58 ± 1.54	248.82 ± 1.81	99.43 ± 1.04
N11	99.39 ± 3.49	0.20 ± 0.11	−6.14 ± 1.31	6.30 ± 0.05	37.32 ± 1.56	228.86 ± 1.12	99.41 ± 1.18
N12	161.93 ± 4.17	0.16 ± 0.004	−4.92 ± 1.10	6.30 ± 0.06	40.53 ± 1.80	209.74 ± 1.78	98.51 ± 2.08
N13	354.96 ± 3.34	0.13 ± 0.03	−3.11 ± 0.65	6.37 ± 0.05	54.63 ± 3.80	282.27 ± 1.89	98.66 ± 2.01
N14	125.53 ± 1.78	0.21 ± 0.01	−5.31 ± 1.52	6.26 ± 0.15	42.41 ± 1.48	327.53 ± 2.68	98.47 ± 2.06
N15	206.00 ± 5.37	0.34 ± 0.004	−3.90 ± 0.63	6.27 ± 0.05	48.53 ± 2.60	293.92 ± 2.94	98.86 ± 2.12

PDI, poly dispersibility index; mV, millivolt; cP, centipoise.

repulsion between droplets that have surface charge, thus preventing the flocculation or coalescence upon random collisions of the particles. While, the steric stability is achieved by the layer formation of steric stabilizer of high molecular weight on the droplets surface which hinders their aggregation (Juniatik et al., 2017).

Table 3 demonstrates the low zeta potential ranges (-12.4 to −3.11 mV) of NE formulations that could be attributed to the ionizable groups (four basic nitrogen atoms) in the structure of CZP that facilitate shifting the zeta potential values toward neutral sign (Venkateswarlu and Manjunath, 2004). In addition, the components of NE used were non-ionic in nature but steric, thus providing a sufficient steric stability in the dispersed phase and retarding Ostwald ripening and coalescence. The hydrophilic groups of the non-ionic surfactants could attract water around them creating a protective barrier that prevented coagulation (Kourniatis et al., 2010). Results revealed that increasing tween 80 concentration would result in globules of smaller sizes with increased surface area and consequently an increase in the surface charges was noticed.

3.4.5. pH measurement

Measuring pH is of a great value as the components used in the formulation can affect the pH of the final preparation and hence determine the route of administration. In addition, change in the pH may affect the zeta potential of the formulation which in turn can influence the stability of preparation. The pH values for all the prepared NEs were within the nasal pH range (5.83–6.47), as presented in Table 3, ensuring their non-irritant nature after intranasal administration (Gaba et al., 2019).

3.4.6. Viscosity measurement

Viscosity plays a crucial role in stability and applicability of intranasal formulations by affecting both the residence time in the nasal cavity and the absorption of drug across the nasal mucosa (Elbardisy et al., 2019). The studied NE formulations demonstrated low viscosity values (12.45–54.63 cP), as shown in Table 3, ensuring the ease of handling, packing and hassle-free administration of NE formulations. The low viscosity might be attributed to the o/w nature of NEs. It was found that increasing tween 80 concentration would decrease the globule size as well as the viscosity of NEs. Results are in accordance with Alanazi et al. (2013).

3.4.7. Solubilization capacity measurement

Table 3 reveals that the solubility of CZP was enhanced in the NE formulations (N8-N15) when compared to its solubility in pure peppermint oil (0.22–1.62 folds). It was clear that the solubility of CZP in the NE formulations increased by increasing the weight ratio of oil and decreased by increasing the weight ratio of water in expense of Smix. The formulation N7 exhibited the lowest solubility of CZP (43.98 ± 1.74 mg/ml) as it contained less amounts of peppermint oil, tween 80 and transcutol P and higher amount of water. Thus, weight ratio of oil:Smix:water had a significant effect on drug solubilization. Our findings were in a good agreement with that reported by Alanazi et al. (2013).

3.4.8. Drug content measurement

All formulations had uniform drug content (∼100%) confirming the efficiency of preparation method and the precision of dose in each formulation (Table 3).

3.4.9. TEM study

Fig. 3 shows representative TEM images of the prepared NEs, in which spherical nanoscale dark droplets with uniform size dispersed with bright background without any agglomeration distinguished throughout the field.

3.4.10. In-vitro drug release study

The *in-vitro* release of CZP from N1-N15 formulations is illustrated in Fig. 4. After 24 h, only 40.93 ± 0.15% of pure CZP was released due to its poor aqueous solubility which was confirmed by the noticed precipitation in the dialysis bag containing CZP suspension. On the other hand, the prepared NE formulations showed a significant higher drug release rate ($p < 0.05$) i.e. >90% in some formulations. The small globule size with subsequent increase in surface area exposed to the release medium, the increased polarity of the formulations by the proper balance between the ratio of oil: Smix and high solubilization capacity of NE formulations were the contributing factors for high drug release (Balata et al., 2016). This could explain the results of N9 formulation (globule size of 83.4 nm, viscosity of 25.84 cP and solubilization capacity of 256.75 mg/ml) which exhibited ∼ 100% drug release within 8 h in comparison to only 57.29% drug release after 24 h exhibited by N7 formulation (globule size of 210.00 nm, viscosity of 51.64 cP and solubilization capacity of 43.98 mg/ml) (Table 3).

Statistical analysis revealed the presence of significant strong positive correlation (Pearson coefficient = 0.9, $p < 0.05$) between the release % and solubilization capacity. In addition, a non-significant negative correlation ($p > 0.05$) was observed between the release % and either globule size or viscosity (Pearson coefficient = -0.1, $p > 0.05$).

The rate and extent of CZP release profile showed no significant difference ($p > 0.05$) between all the prepared NE formulae (Prabhakar et al., 2013). Therefore, N9 and N3 were selected as optimum formulations because of their high release profile, small globule size (<100 nm), suitable zeta potential and low viscosity. It was reported that small particle size (<100 nm) is a critical factor for the intranasal delivery of drugs to the CNS as it exhibits larger surface area with enhancement of the rate of drug absorption through olfactory and trigeminal nerve terminations (Bayanati et al., 2021).

3.4.11. Release kinetic analysis

As shown in Table 4, the *in-vitro* release data were analyzed according to several kinetic models. The higher R^2 values for first order kinetics than zero order kinetics were obtained indicating that the release of CZP from NEs was concentration dependent (Arora et al., 2014). To analyze the release mechanism of drug from NE formulations, the data were fit to Korsmeyer-Peppas model (R^2 >0.95). The release exponent (n) ranged between 0.5 and 1 indicating non-Fickian/anomalous release of CZP from the studied NE formulations (Zaki et al., 2007).

3.4.12. Stability studies

Table 5 illustrates the different parameters tested along the storage period including physical appearance, % transmittance, pH, viscosity, drug content, globule size, PDI and zeta potential. The studied formulations showed clear, light and transparent appearance. The results revealed that the selected N3 and N9 formulations were physically stable at room temperature and at 4 °C for a period of 3 months without phase separation, creaming or cracking. It is clear that all the tested parameters showed no significant change by storage confirming the absence of any serious chemical reactions that could negatively impact the quality of the tested preparations with decreased Ostwald ripening rate (Moradi and Barati, 2019). This may be due the proper selection of NE components where short chain oils such as peppermint oil are capable of overcoming this problem due to its steric property (Aiswarya et al., 2015). Additionally, Abdul Aziz et al., 2019 pointed out the use of tween 80, as a non-ionic surfactant, can assist in formation of a viscoelastic interfacial film at the o/w interface thus preventing the droplets coalescence.

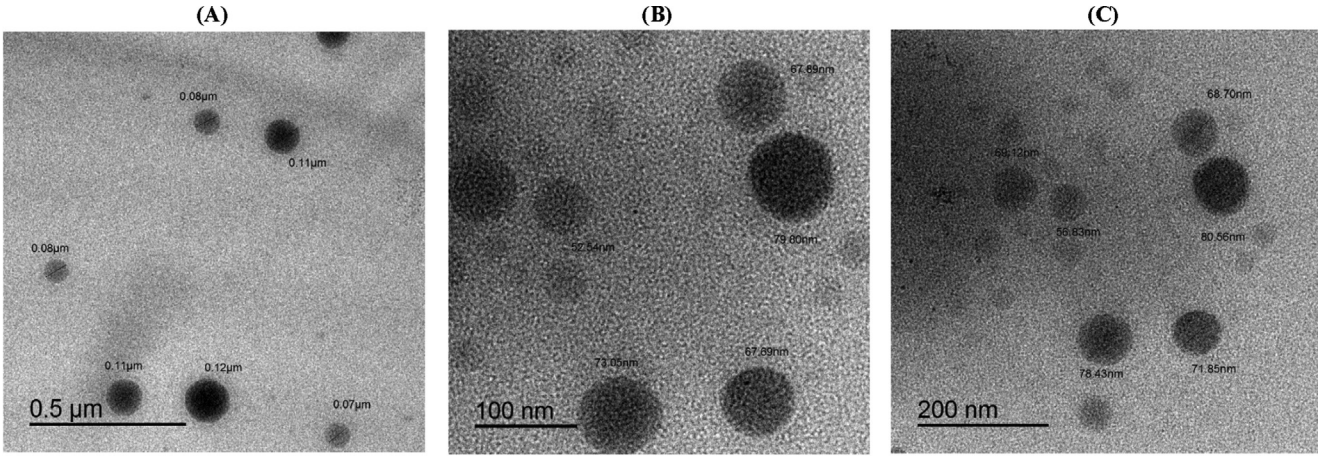

Fig. 3. TEM images of NE at different scales (A) 0.5 µm (B) 100 nm (C) 200 nm.

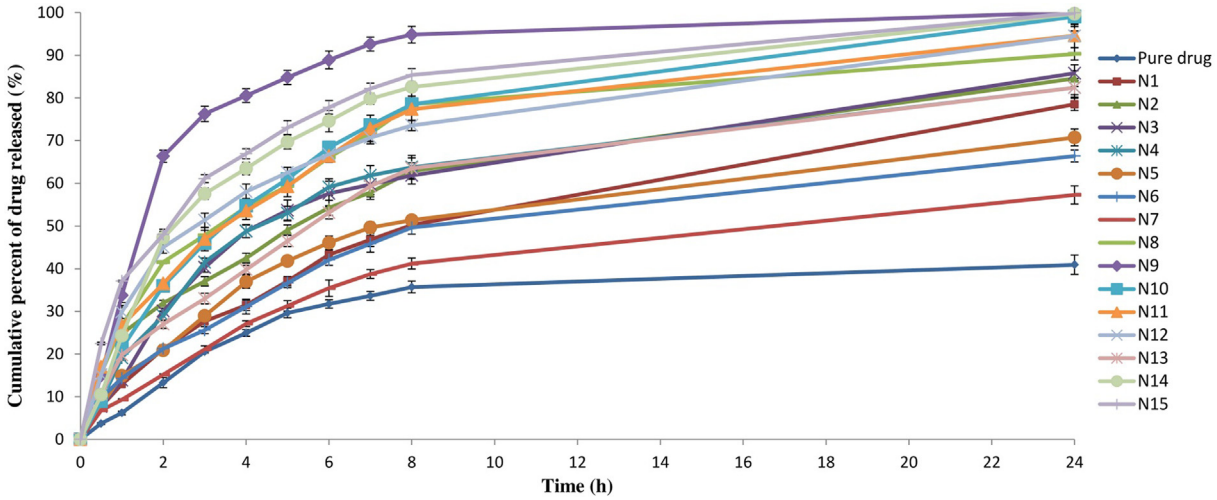

Fig. 4. *In-vitro* release of different CZP-loaded NE formulations (N1-N15) in comparison to pure drug suspension.

Table 4
Correlation coefficient (R^2) values of different kinetic release profiles.

Formula	Zero order	First order	Higuchi	Hixson-Crowel	Korsmayer-Peppas	
	R^2	R^2	R^2	R^2	R^2	n
Pure drug	0.9411	0.9720	0.9207	0.9642	0.9734	0.753
N1	0.9590	0.9770	0.9195	0.9751	0.9793	0.789
N2	0.9443	0.9804	0.9503	0.9717	0.9897	0.713
N3	0.8822	0.9732	0.9461	0.9555	0.9770	0.641
N4	0.8616	0.9742	0.9800	0.9501	0.9885	0.584
N5	0.9342	0.9798	0.9544	0.9706	0.9875	0.692
N6	0.9117	0.9640	0.9781	0.9512	0.9955	0.632
N7	0.9599	0.9817	0.9289	0.9772	0.9849	0.773
N8	0.8319	0.9274	0.9698	0.9045	0.9736	0.557
N9	0.6481	0.9848	0.9453	0.9633	0.9491	0.552
N10	0.8975	0.9935	0.9764	0.9803	0.9926	0.623
N11	0.8440	0.9622	0.9920	0.9408	0.9950	0.549
N12	0.6009	0.9853	0.9796	0.8206	0.9969	0.503
N13	0.9244	0.9695	0.9658	0.9617	0.9895	0.660
N14	0.7994	0.9753	0.9721	0.9465	0.9758	0.537
N15	0.6497	0.9536	0.9852	0.9025	0.9942	0.528

n, release exponent.

Table 5
Stability study of stored selected NE formulations (N3 and N9).

Formula	Time (month)	% transmittance		pH		Viscosity (cP)		Drug content (%)		globule size (nm)		PDI		Zeta potential (mV)	
		At 4 °C	At 25 °C	At 4 °C	At 25 °C	At 4 °C	At 25 °C	At 4 °C	At 25 °C	At 4 °C	At 25 °C	At 4 °C	At 25 °C	At 4 °C	At 25 °C
N3	0	99.99 ± 0.22	99.98 ± 0.10	6.30 ± 0.03	6.43 ± 0.05	19.37 ± 1.68	18.42 ± 3.80	99.98 ± 1.01	100.03 ± 0.17	73.82 ± 2.43	73.82 ± 2.43	0.24 ± 0.03	0.24 ± 0.03	−11.40 ± 0.40	−11.40 ± 0.40
	1	99.85 ± 1.34	99.96 ± 1.23	6.32 ± 0.03	6.43 ± 0.12	19.41 ± 1.50	18.63 ± 2.51	99.93 ± 1.01	99.99 ± 1.04	74.85 ± 2.92	73.96 ± 2.76	0.26 ± 0.04	0.26 ± 0.04	−11.23 ± 0.32	−11.35 ± 0.36
	2	99.91 ± 1.79	99.94 ± 1.58	6.31 ± 0.12	6.46 ± 0.34	19.39 ± 2.41	18.50 ± 1.62	99.96 ± 1.12	99.98 ± 1.32	75.35 ± 3.09	74.48 ± 3.12	0.29 ± 0.15	0.26 ± 0.11	−10.54 ± 0.48	−11.28 ± 0.35
	3	98.98 ± 0.36	99.97 ± 1.53	6.30 ± 0.05	6.47 ± 0.16	19.43 ± 1.78	18.53 ± 1.26	99.96 ± 1.23	99.98 ± 1.59	76.17 ± 3.19	75.23 ± 3.15	0.31 ± 0.17	0.30 ± 0.14	−9.76 ± 0.53	−10.36 ± 0.47
N9	0	98.91 ± 1.38	98.93 ± 0.45	6.38 ± 1.20	6.40 ± 0.10	26.34 ± 1.38	25.84 ± 0.23	99.98 ± 1.43	100.13 ± 1.06	83.40 ± 3.89	83.40 ± 3.89	0.14 ± 0.03	0.14 ± 0.03	−12.40 ± 1.73	−12.40 ± 1.73
	1	98.93 ± 1.42	99.91 ± 1.54	6.41 ± 1.53	6.43 ± 1.20	26.41 ± 2.73	25.81 ± 1.20	99.95 ± 2.45	99.97 ± 1.62	84.54 ± 3.74	83.58 ± 3.92	0.13 ± 0.02	0.15 ± 0.04	−11.87 ± 1.65	−12.60 ± 1.65
	2	98.97 ± 2.53	98.87 ± 2.72	5.99 ± 1.41	6.42 ± 1.57	26.63 ± 1.85	26.13 ± 2.63	99.91 ± 1.62	99.95 ± 1.71	85.36 ± 3.18	84.79 ± 4.12	0.17 ± 0.08	0.19 ± 0.08	−11.13 ± 1.87	−11.97 ± 1.58
	3	98.89 ± 1.69	98.91 ± 0.35	6.26 ± 1.37	6.41 ± 1.48	26.47 ± 2.49	25.99 ± 2.57	99.89 ± 2.39	99.96 ± 1.21	86.82 ± 4.67	85.34 ± 4.36	0.21 ± 0.14	0.22 ± 0.12	−10.46 ± 1.86	−11.13 ± 1.72

3.5. Preliminary studies for measurement of Tsol-gel and GT and preparation of NGs

Ideally, an *in-situ* gelling system should contain a low viscous fluid to allow a nasal reproducible administration and transform into a gel of higher viscosity at 31 °C according to the reported average temperature in human nose (Okur et al., 2020; Qian et al., 2014). Thus, the increased viscosity would lower the mucociliary clearance and extend the residence time within the nasal cavity (Qian et al., 2014). As a result, optimizing Pluronic® concentration was a necessity to achieve a desired Tsol-gel (Fakhari et al., 2017). Therefore, preliminary attempts were made to optimize the polymer concentration used to form a gel at such temperature.

Pluronic F-127, an efficacious thermosensitive polymer, can be converted from solution to gel state by increasing temperature. It is reported that PF127 is more soluble in cold water, so the cold method was employed for *in-situ* gel preparation (Escobar-Chávez et al., 2006). PF127 polymer can form gel with aqueous pores at its Tsol-gel. Although the 3D network of the formed hydrogel is sufficiently rigid, the highly hydrated microscale medium can boost the mass transfer and release of both hydrophilic and hydrophobic drugs via the extramicellar water channels (Anderson et al., 2001). At sufficiently high concentration and temperature, PF127 can be able to form micelles which can pack together in a highly ordered structure lattice which is the driving force for gelation (Bonacucina et al., 2011). Results of Table 6 revealed that out of the various examined polymer concentrations; only a concentration of 20% w/w could exhibit a Tsol-gel at 30.24 ± 1.83 °C which was suitable for the nasal administration and hence was selected for incorporation of the selected NE formulations. There was an inverse relationship between the polymer concentration and Tsol-gel value. These results were in agreement with Chen et al. (2010).

However, incorporation of NEs resulted in lowering the Tsol-gel which was in agreement with that reported by Basu and Bandyopadhyay (2010); Zaki et al. (2007). It was observed that upon addition of NE to the gel base at ratios of 1:1 and 1:2, no gelation occurred and when the NE:gel ratio was increased to 1:3, 1:4 and 1:5, the Tsol-gel values were 28.53 ± 1.34, 26.85 ± 1.45 and 25.32 ± 1.12 °C respectively, which were not within the targeted region of *in-situ* gelation (Table 6). Thus, PF127 could not be used alone and the addition of another polymer was a necessity to raise the Tsol-gel. This could be attributed to the structure of PF127 comprising 70% hydrophilic polyethylene oxide (PEO) units and 30% hydrophobic polypropylene oxide (PPO) units. As the dehydration of hydrophobic PPO block could facilitate its gelation, reducing the ratio of PPO to PEO would enhance the entanglement of adjacent molecules associated with more extensive intermolecular hydrogen bonding, hence increasing the Tsol-gel of PF127. Therefore, using PF68 polymer comprising low PPO ratio (16%) could efficiently raise the Tsol-gel of PF127-based thermosensitive *in-situ* gels (Al Khateb et al., 2016). Similar results were reported by Abd ElHady et al. (2003); Kolsure and Rajkapoor (2012).

As shown in Table 6, combinations of PF127 (20% w/w) with different concentrations of PF68 (1–5% w/w) were studied. It was clear that a combination of PF127 and PF68 at 20:2% w/w was appropriate with an acceptable Tsol-gel at 31.98 ± 1.64 °C. Similar results were obtained by Velupula and Janapareddi (2019). Incorporation of the selected N3 and N9 formulations to this combination at NE:gel ratio<1:3 resulted in no gelation. While, increasing the NE:gel ratio to 1:3, 1:4 and 1:5 w/w resulted in increasing the Tsol-gel values to 30.21 ± 1.34, 30.97 ± 2.67 and 31.58 ± 2.41 °C, respectively. In addition, different prepared solution-gel formulations exhibited short gelation time (GT) ~ 30 s confirming their capability of rapid gel formation after nasal administration

Table 6
Preliminary studies for measurement of Tsol-gel and GT and preparation of NG formulations.

Formula	Gel composition (% w/w)		Ratio of NE:gel	Tsol-gel (°C)	GT (s)
	PF127	PF68			
G1	18	–	–	37.82 ± 1.54	50.33 ± 1.53
G2	19	–	–	33.82 ± 1.67	46.67 ± 2.08
G3	20	–	–	30.24 ± 1.83	50.33 ± 1.53
G4	21	–	–	27.54 ± 2.01	45.67 ± 2.08
G5	22	–	–	24.87 ± 1.64	43.00 ± 3.00
G6	23	–	–	20.34 ± 1.21	41.33 ± 1.53
NE + G3 (1:1)	20	–	1:1	No gelation	
NE + G3 (1:2)	20	–	1:2	No gelation	
NE + G3 (1:3)	20	–	1:3	28.53 ± 1.34	30.33 ± 1.15
NE + G3 (1:4)	20	–	1:4	26.85 ± 1.45	30.33 ± 1.53
NE + G3 (1:5)	20	–	1:5	25.32 ± 1.12	28.00 ± 2.00
G3 + PF68 (1%)	20	1	–	30.54 ± 1.32	30.00 ± 2.00
G3 + PF68 (2%)	20	2	–	31.98 ± 1.64	33.33 ± 1.53
G3 + PF68 (3%)	20	3	–	33.71 ± 1.62	35.67 ± 3.00
G3 + PF68 (4%)	20	4	–	34.56 ± 1.81	39.33 ± 3.05
G3 + PF68 (5%)	20	5	–	35.32 ± 2.44	43.00 ± 3.00
NG1	20	2	1:1	No gelation	
NG2	20	2	1:2	No gelation	
NG3	20	2	1:3	30.21 ± 1.34	27.33 ± 2.52
NG4	20	2	1:4	30.97 ± 2.67	29.67 ± 1.53
NG5	20	2	1:5	31.58 ± 2.41	30.00 ± 1.00

PF127, Pluronic® F-127; PF68, Pluronic® F-68; NE, nanoemulsion; Tsol-gel, solution-gel temperature; GT, gelation time.
* Water was added to the PF127 and PF68 polymeric bases up to 100% w/w.
* There were no significant differences between results of incorporation of N3 or N9 into the tested gels.

(Qian et al., 2014). Therefore, NG3 formulation comprising 1:3 ratio of NE:gel mixture was found to be suitable for *in-situ* gel preparation and was selected for further studies.

Moreover, the influence of addition order of Pluronics® was also investigated. When the polymers were added directly to NE formulations, tiny agglomerates were observed due to improper swelling. On the contrary, when the polymers were swollen in aqueous phase and added to NE formulation, a homogenous NG was obtained but the produced gel was transluscent or slightly turbid. While, the addition of NE to the swollen gel resulted in a homogenous clear transparent gel (Mahaparale and Gaware, 2017). Arora et al. (2014) reported that the order of addition of Pluronics® influenced the homogeneity of gel matrix.

3.6. Characterization of CZP-loaded NGs

3.6.1. Visual assessment for clarity

Evaluation of gel formulations for clarity, homogeneity and grittiness by either visual or microscopic observation, confirmed the desired requirements for intranasal formulations of being clear homogenous and free from any undissolved particulates (Mahaparale and Gaware, 2017).

3.6.2. pH measurement

The pH values were 6.35 ± 0.52 and 6.41 ± 0.71 for NG3 formulations containing N3 and N9, respectively, which were in the range of nasal physiologic pH. This pH favored non-irritant adherence to the nasal mucosa producing intermediate permeation release rate with sustained effect (Naeem et al., 2015).

3.6.3. Viscosity measurement

Viscosity plays a vital role while optimizing the intranasal formulations as it controls their flowability, spreadability, release of drug and residence time in the nasal mucosa (Arora et al., 2014; Gaba et al., 2019). NG3 formulations containing either N3 or N9 exhibited low viscosity values at room temperature (320.92 ± 4.9 7 cP and 435.75 ± 6.64 cP, respectively) as the gel formulations were in liquid form. However, upon increasing the temperature to 31 °C, the formulations converted to gel texture and the viscosity increased. NG3 formulation containing N3 demonstrated viscosity of 783.64 ± 11.22 cP which was two thirds the viscosity of that containing N9 (1167.48 ± 19.14 cP).

3.6.4. Gel strength measurement

Results of gel strength for the optimal formulations NG3 containing N3 and N9 were 33.45 ± 3.43 and 41.62 ± 2.68 s, respectively. The results were in agreement with Hosny and co-workers (2020) who reported that the ideal gel strength value between 25 and 50 s is sufficient to ease the gel administration and prevent its leakage out of the nasal cavity. Preparations having gel strength values below 25 s erode rapidly due to insufficient integrity, while those exceeding 50 s are very stiff and uncomfortable upon use. Thus, gel strength values were within the acceptable range.

3.6.5. Spreadability measurement

Good spreadability is an essential criteria for the NG formulations. It reveals the ease of application and delivery of the correct dose of loaded drug (Mbah et al., 2019). In our study, there was inverse relationship between gel viscosity and spreadability. At 25 °C, the prepared NG3 containing N3 and N9 exhibited low viscosity and high spreadability (8.50 ± 0.15 and 7.30 ± 0.21 cm, respectively). While at 31 °C, the two formulations had higher viscosity with less spreadability values (5.40 ± 0.87 and 4.60 ± 0.12 c m, respectively). Similar results were reported by Chaudhary and Verma (2014); Morsy et al. (2019).

3.6.6. In-vitro drug release from selected NGs

Fig. 5 demonstrates the release pattern of CZP from the selected NGs compared to their corresponding NE formulations and the control gel. About 60–70% of drug released from the selected NGs was observed within the first 8 h compared to only 20% from the control gel, then followed by a sustained release pattern for 24 h. The low release pattern of CZP from the control gel formulation might be related to the low CZP aqueous solubility and the subsequent low dissolution (Sayed et al., 2021). Slower release rate of CZP was observed from NE-based gels when compared to that from their corresponding NE formulations owing to several factors: 1) entrapment of CZP in the oil phase which necessitated drug release

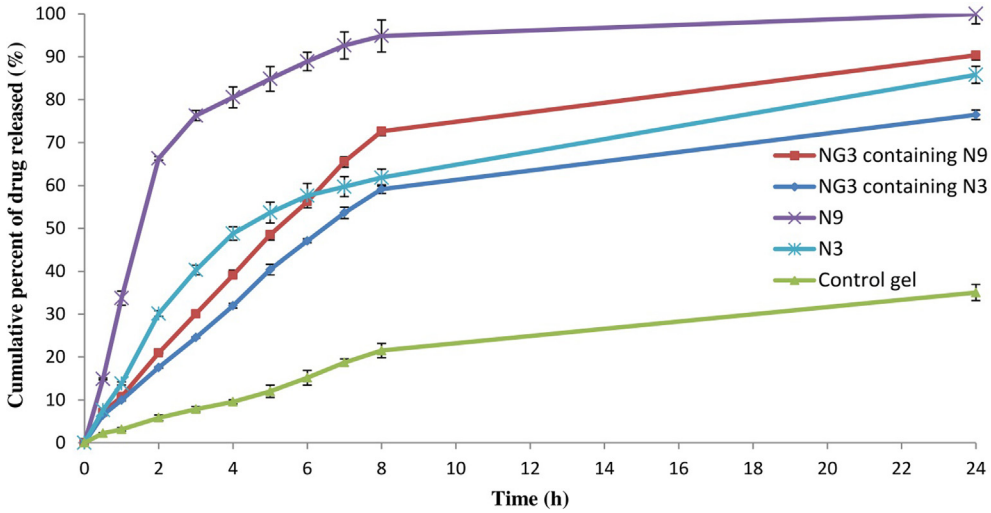

Fig. 5. *In-vitro* release of CZP-loaded NG3 formulations containing N9 and N3 compared to their corresponding NE formulations and control gel formulation.

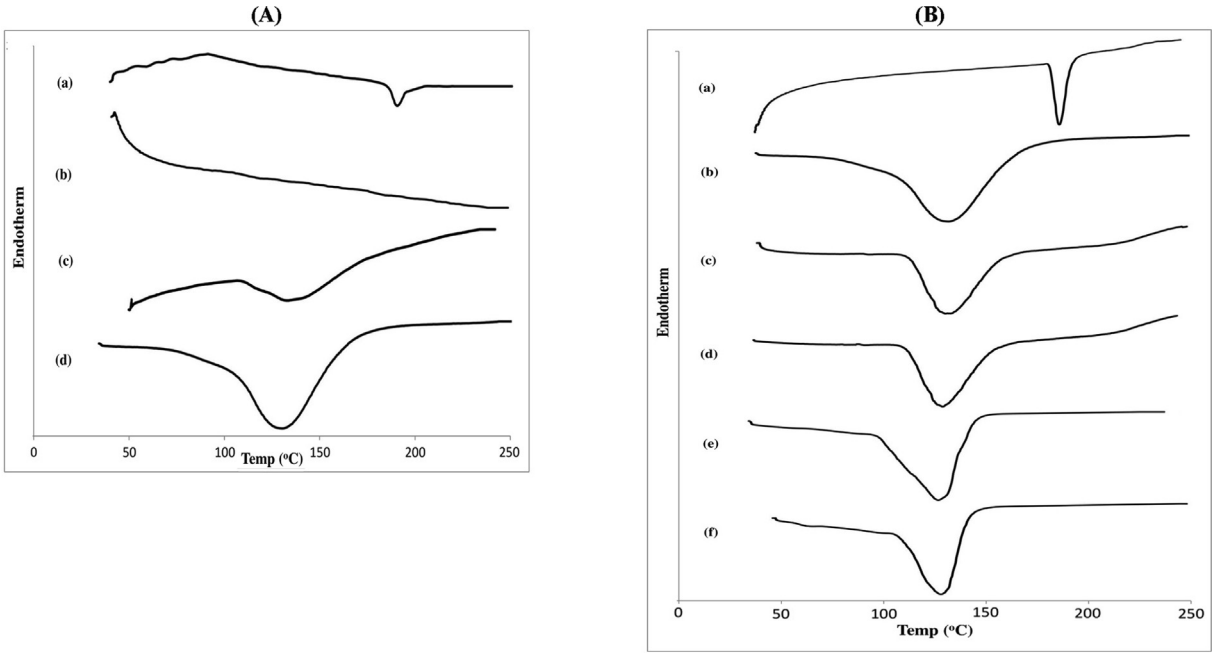

Fig. 6. (A) DSC thermograms of (a) peppermint oil (b) tween 80 (c) transcutol P (d) blank NE.
(B) DSC thermograms of (a) pure CZP (b) blank NE (c) N3 (d) N9 (e) NG3 containing N3 (f) NG3 containing N9.

first from oil into the interfacial layer and then into the aqueous phase, 2) addition of Pluronic® polymers led to increased surfactant concentration, which restricted the diffusion of drug to the release medium, 3) Pluronic® polymers had a core–shell structure where the hydrophobic core as a drug-loading site along with the hydrophilic outer shell resulted in slow release of CZP, 4) enhancement of viscosity due to the formation of 3D gel network (Arora et al., 2014; Chaudhary and Verma, 2014; Russo and Villa, 2019). Therefore, NGs would be favored based on the applicability view point.

3.6.7. DSC study of selected NE and NG formulations

The DSC thermograms of pure CZP, NE components, selected NE and selected NG formulations are illustrated in Fig. 6. The DSC thermogram of pure CZP showed a sharp endothermic peak at 181.24 °C which was corresponding to its melting point. The sharpness of the peak indicates the crystallinity and purity of CZP (Velupula and Janapareddi, 2019). The DSC thermograms of peppermint oil and transcutol P showed tiny endothermic peaks at 179.77 and 126.69 °C respectively, while tween 80 showed no peak (Fig. 6A). The thermal behavior of the NE and NG formulations showed the absence of characteristic CZP peak with predominance of NE peak (Fig. 6B). This result was explained on the basis of molecular dispersion of drug in the oil phase of NE and increased drug solubilization capacity by NE preparation (Gaba et al., 2019).

3.6.8. FTIR study of selected NE and NG formulations

Fig. 7 illustrates the FTIR spectra of pure CZP, NE components, selected NE and selected NG formulations. The spectrum of pure CZP showed N-H stretching peak at 3449 cm^{-1}, C-H stretching aro-

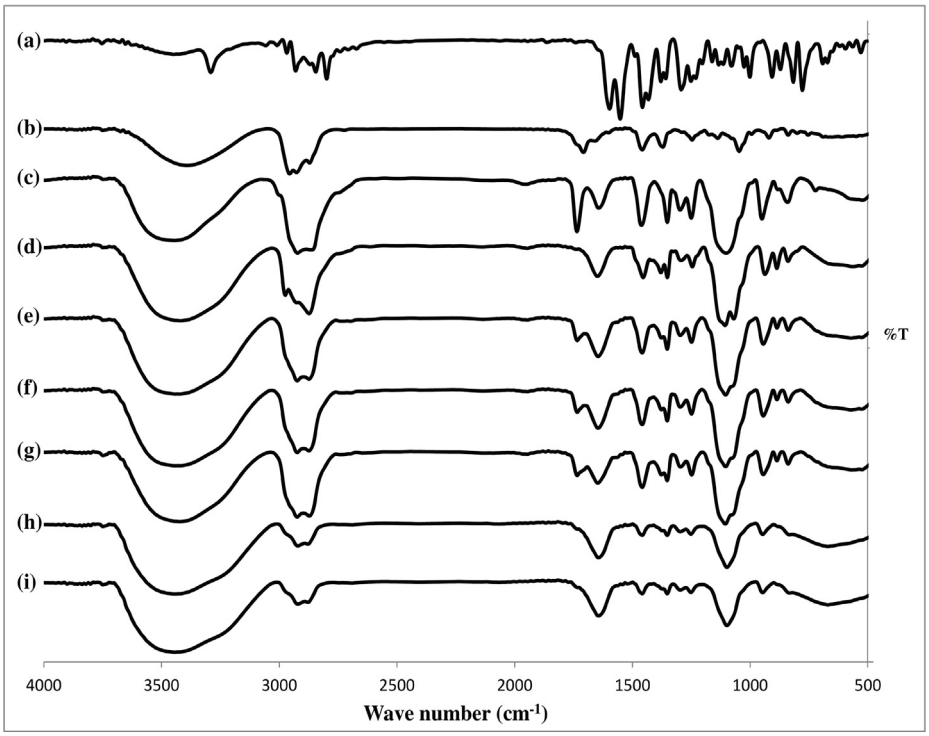

Fig. 7. FTIR spectrums of (a) pure CZP (b) peppermint oil (c) tween 80 (d) transcutol P (e) blank NE (f) N3 (g) N9 (h) NG3 containing N3 (i) NG3 containing N9.

matic peak at 3291 cm^{-1}, C-H stretching aliphatic peaks at 2931 and 2845 cm^{-1}, C = N stretching peaks at 1597 and 1552 cm^{-1}, C = C stretching aromatic peaks at 1457 and 1432 cm^{-1}, C-N stretching peak at 1293 cm^{-1} due to tertiary amine, and C-CL stretching peak at 816 cm^{-1}. The FTIR spectrums of peppermint oil and tween 80 showed stretching peaks for O-H bonding (3391 and 3445 cm^{-1}), C-H aliphatic vibrations (2956, 2927 and 2923, 2861 cm^{-1}), carbonyl vibrations (1708 and 1736 cm^{-1}) and C-O vibrations (1046 and 1102 cm^{-1}). Transcutol P spectrum showed the same stretching vibration peaks except those of the carbonyl group.

FTIR spectrum of peppermint oil showed absorption band of O-H group forming hydrogen bond with N-H of CZP which might explain the increased solubility of CZP in peppermint oil. This assumption was approved by the FTIR spectrum of the NE formulations (Fig. 7B: f and g) which showed the absence of the characteristic peak of N-H group of CZP and the broadness of the O-H peak. Moreover, the reduced peak strength of aromatic C-H group peak and aromatic C = C group in the FTIR spectrum of the NE formulations confirmed the good interaction of CZP with the liquid vehicles since the concentration percentage of CZP became very low when compared to that of liquid vehicles alone. FTIR spectrum of tween 80 represented a sharp peak of C = O group reflecting the presence of dipole–dipole interaction with CZP induced by electrostatic attraction. These interactions in addition to the hydrogen bonding lead to sustained action of the formulation. Transcutol P had many ether bonds which suggested a possible reaction with CZP by the formation of weak hydrogen bonds with the available proton of secondary amine or vander-waals interaction with the far tertiary amine of CZP with low steric hindrance. FTIR results outline the capability of peppermint oil, tween 80 and transcutol P to generate new chemical bondings with CZP which explained reasonable enhancement of CZP solubility. On another hand, the FTIR spectra of specific groups of the NG components explained their ability to form intermolecular hydrogen bondings with free O-H groups of the bulky molecule, tween 80, present in the NE formulation. This result was approved by the FTIR spectrum of the NG formulations (Fig. 7B: h and i). These results could propose the homogenous mixing and incorporation of CZP in the investigated components with absence of chemical interactions (Ibrahim et al., 2018).

3.6.9. Ex-vivo permeation data analysis

Fig. 8 shows the *ex-vivo* permeation study of CZP through the nasal mucosa which was slower than that through the artificial membrane due to the major barrier effect exerted by the biological membrane (Mura et al., 2014). CZP-incorporated NG formulations showed significant enhanced permeation compared with the control gel with superior permeation for those containing N9 than N3 formulations (Fig. 8 and Table 7). This result could be attributed to many factors. First, nanosized globules increased drug solubilization and surface area exposed for drug permeation through nasal mucosa (Morsy et al., 2019). Second, the formulation components presented their ability to disrupt the lipidic bilayer. Many reports mentioned the ability of tween 80 to enhance the drug permeability via nasal mucosa (Gaba et al., 2019; Morsy et al., 2019). In addition, transcutol P was highly associated with facilitating CZP penetration through the biological membranes by its ability to incorporate into the multiple lipid bilayers of the membrane with subsequent swelling of intercellular lipids (Elshafeey et al., 2009). Aggarwal et al. (2013) reported that transcutol P was able to alter the structure of the biological membranes by lipid extraction and hence increase the permeability of the drug. Moreover, Pluronics® architecture has an influence on drug transportation by enhancing drug retention and permeability. They promote sustained drug release by incorporation of lipophilic drugs in the core of their micelles (Russo and Villa, 2019). Third, the viscosity of the formulation could affect the drug absorption across the nasal mucosa as reported by Furubayashi et al. (2007); Idrees et al. (2011). They mentioned that increasing the viscosity of formulations caused a decrease in drug penetration rate across the mucus layer with subsequent delay in the drug reaching to cellular surfaces.

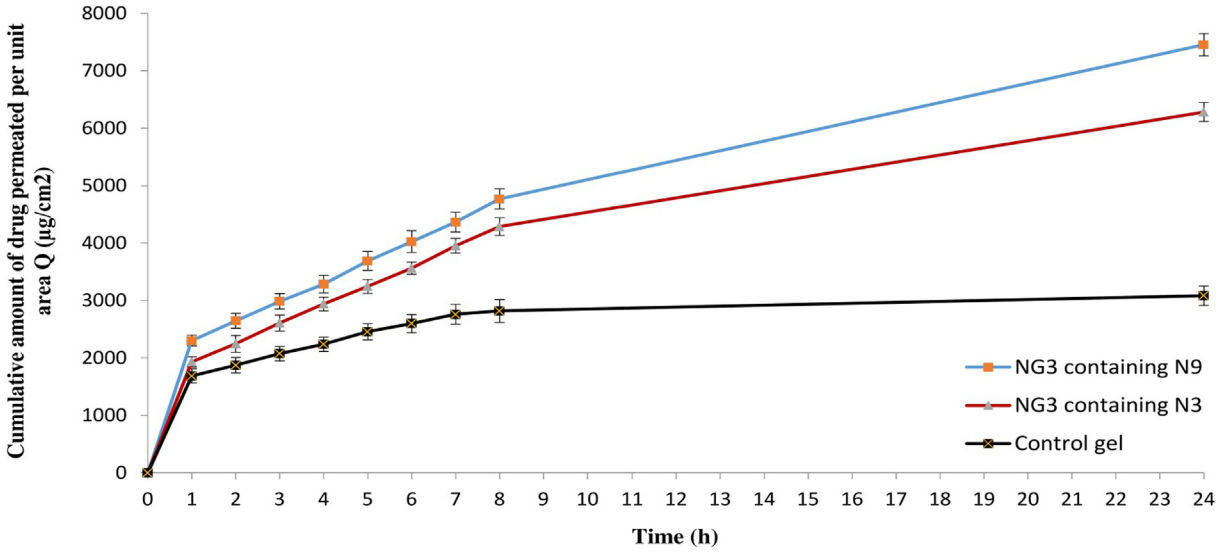

Fig. 8. *Ex-vivo* permeation of NG3 containing either N9 or N3 in comparison to control gel formulation.

Table 7
Ex-vivo permeation parameters of NG3 containing either N9 or N3 in comparison to control gel formulation.

Permeation parameters	NG3 containing N3	NG3 containing N9	Control gel
Jss ($\mu g/cm^2.h^{-1}$)	335.71 ± 23.64	350.04 ± 20.29	175.97 ± 16.25
Kpx10^{-3} (cm/h)	13.43 ± 2.45	14.00 ± 3.81	8.80 ± 3.94
Er	1.91	1.99	–
Drug deposited in mucosa (mg)	3.45 ± 1.34	4.76 ± 1.87	1.83 ± 0.32

Jss, drug flux at steady state; Kp, permeability coefficient; Er, enhancement ratio.

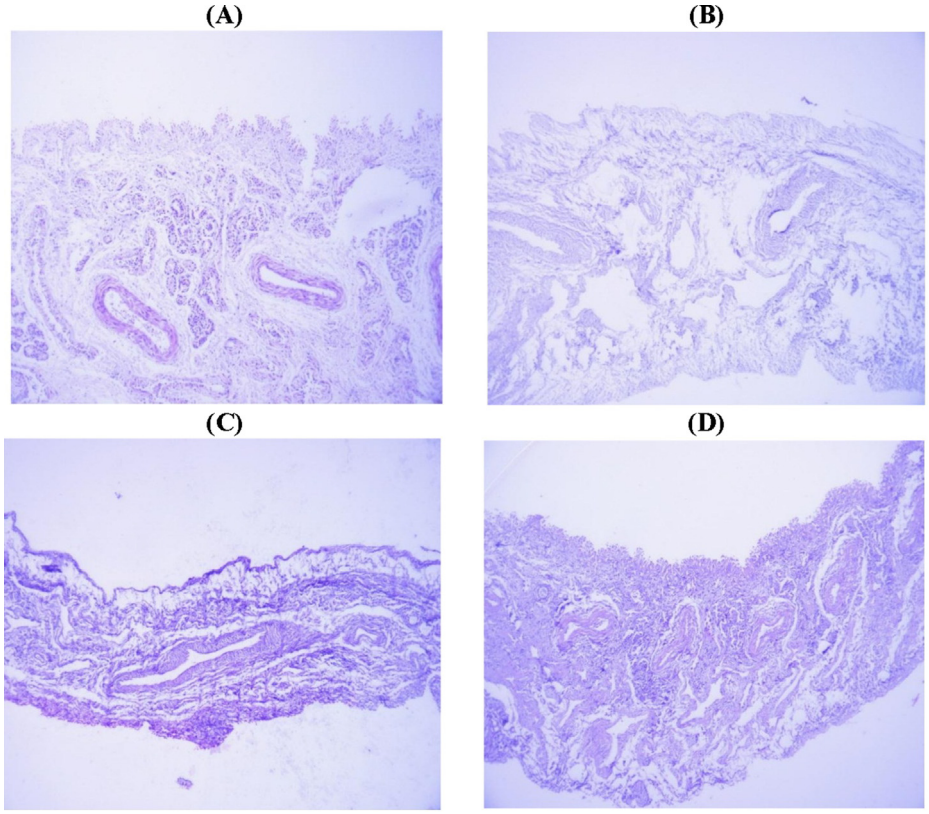

Fig. 9. Nasal cilotoxicity study of sheep nasal mucosa treated with (a) saline (b) isopropyl alcohol (c) NG3 containing N3 (d) NG3 containing N9.

Table 8
Stability studies of stored selected NG formulations.

Formula	Time (month)	Physical appearance		Tsol-gel (°C)		pH		Viscosity (cP)		Gel strength (s)		Spreadability (cm)	
		At 4 °C	At 25 °C	At 4 °C	At 25 °C	At 4 °C	At 25 °C	At 4 °C	At 25 °C	At 4 °C	At 25 °C	At 4 °C	At 25 °C
NG3 containing N3	**0**	Clear and homogeneous with no grittiness		–	30.21 ± 1.34	6.37 ± 0.84	6.35 ± 0.52	320.67 ± 13.65	320.92 ± 14.97	33.42 ± 2.58	33.45 ± 3.43	5.40 ± 2.43	5.40 ± 2.87
	1			29.80 ± 0.53	29.80 ± 0.32	6.35 ± 0.61	6.38 ± 0.15	318.73 ± 12.69	318.32 ± 14.23	33.45 ± 2.64	33.48 ± 2.12	5.46 ± 1.34	5.48 ± 2.71
	2			29.70 ± 0.61	29.70 ± 0.86	6.35 ± 0.12	6.35 ± 0.35	317. 61 ± 12.63	316.41 ± 12.64	33.61 ± 2.53	33.57 ± 2.16	5.71 ± 1.78	5.62 ± 1.63
	3			29.60 ± 0.97	29.60 ± 1.21	6.36 ± 0.12	6.36 ± 0.24	315.78 ± 12.93	314.72 ± 13.75	33.64 ± 2.34	33.67 ± 2.65	5.73 ± 1.55	5.68 ± 1.37
NG3 containing N9	**0**	Clear and homogeneous with no grittiness		–	30.21 ± 1.34	6.40 ± 0.23	6.41 ± 0.71	435.31 ± 6.37	435.75 ± 6.46	40.58 ± 2.34	41.62 ± 2.68	4.61 ± 1.20	4.60 ± 1.12
	1			29.80 ± 1.32	29.80 ± 1.12	6.41 ± 0.31	6.40 ± 0.12	437.64 ± 6.12	439.23 ± 6.86	40.95 ± 2.54	41.73 ± 3.66	4.58 ± 1.32	4.61 ± 0.76
	2			29.70 ± 0.56	29.50 ± 0.61	6.37 ± 0.05	6.40 ± 0.001	439.82 ± 8.36	440.71 ± 9.63	41.44 ± 3.84	42.16 ± 3.56	4.62 ± 1.13	4.62 ± 0.97
	3			29.50 ± 0.52	29.40 ± 0.73	6.40 ± 0.001	6.37 ± 0.02	441.39 ± 9.85	442.68 ± 9.75	41.98 ± 4.32	42.87 ± 3.67	4.62 ± 1.30	4.63 ± 1.24

3.6.10. Mucoadhesive strength study

The mucoadhesive strength values of NG3 containing N3 and N9 were 4867.41 ± 86.52 and 5185.00 ± 97.41 dyne/cm^2, respectively, having 1.55–1.65 folds increase than that of the control gel (3135.00 ± 21.45 dyne/cm^2). Wang et al. (2017) reported that formulations of mucoadhesive strength values within range of 4000–6000 dynes/cm^2 are acceptable for nasal administration. Satisfactory mucoadhesive strength can enhance the formulations residence time in nasal cavity, restrict their clearance and therefore prolong drug release (Chaudhary and Verma, 2014). On the other hand, excess mucoadhesive strength may damage the mucous membrane. Therefore, optimum strength values are required for administration of gels into the nose.

Generally, the mucoadhesive effect of Pluronic® polymers is related to their amphiphilic nature which facilitates their interpenetration into the mucus where forming entanglements or non-covalent bonds by the Van der Waals and hydrogen forces that result in their adhesion of to the nasal mucosa (Fakhar-Ud-Din and Khan, 2017). Enhanced mucoadhesive properties of CZP-loaded NGs might be attributed to the synergistic action of thermally-induced adsorption of Pluronic® polymers onto the NE droplet interface and an increased Pluronic® micelle formation in the continuous aqueous phase. There are multiple hydrophobic sites that enhance the self-assembly of Pluronic® molecules as temperature rises, that include the NE oil droplets and the hydrophobic core of tween 80 micelles. This strong interaction leads to increased gel viscosity and strength (Hashemnejad et al., 2019).

Our findings were in agreement with Bayanati et al., 2021 who found that the mucoadhesive percentage of the formulated NE-loaded *in-situ* gels using PF127 and PF68 polymers was higher than that of the drug solution-loaded *in-situ* gels owing to the viscosity of the NE formulations that led to increased residence time of temozolomide in the nasal cavity. In addition, Wong et al. (2013) studied the effect of surfactant composition on mucoadhesion of intranasal NE and reported that the non-ionic interaction between NE ingredients (tween 80) and major protein (mucin) in mucus had a potential effect on mucoadhesive strength.

3.6.11. Nasal ciliotoxicity study

The nasal ciliotoxicity study was performed to investigate whether CZP-loaded NG components could yield any potential toxic effects on the nasal mucosa (Chaudhary and Verma, 2014). Histopathological study of nasal mucosa revealed that the epithelial layers of saline-treated mucosal pieces remained intact with no nasociliary damage or inflammation signs such as erythema or edema (Fig. 9A). While, the isopropyl alcohol-treated pieces showed destructed nasal cilia with extensive mucosal damage (Fig. 9B).

Regarding those of the selected NG formulations, the epithelial layers remained intact without any signs of toxicity (Fig. 9: C and D). The observed minor changes of mucosa including loss of some epithelium parts and congestion of vessels were exhibited normally due to the separation and cutting procedures (Sita and Vavia, 2020). This result was in agreement with previous report of Gaba et al. (2019) regarding the safety and biocompatibility of the investigated components.

3.6.12. Stability studies of selected NGs

Results of stability study of the selected NG formulations are summarized in Table 8. It was clear that NG formulations were stable upon storage for 3 months with no significant changes in their physical appearance, Tsol-gel, pH, viscosity, gel strength and spreadability. This result was in agreement with Shah et al. (2019).

4. Conclusions

CZP, anti-schizophrenic drug, can be effectively incorporated in o/w NEs composed of peppermint oil, tween 80, transcutol P with optimal ratio of Smix (1:1) and oil:Smix ratios of 1:7 (N3) and 2:7 (N9). Because of the appropriate viscosity of the prepared NEs, they can be effectively incorporated in thermosensitive *in-situ* gels composed of a combination of PF127 and PF68 at 20:2% w/w at NE:gel ratio of 1:3. The prepared gels showed acceptable physical properties in terms of appearance, viscosity and spreadability as well as nasal permeation properties. NE-based *in-situ* gels may be a promising and biocompatible dosage form for intranasal administration of CZP.

Funding

This research did not receive any specific grant from funding agencies in the public, commercial, or not-for-profit sectors.

Declaration of Competing Interest

The authors declare that they have no known competing financial interests or personal relationships that could have appeared to influence the work reported in this paper.

References

Abd Elhady, S.S., Mortada, N., Awad, G.A.S., Zaki, N.M., Taha, R.A., 2003. Development of in situ gelling and mucoadhesive mebevarine hydrochloride solution for rectal administration. Saudi Pharm. J. 11, 159–171.

Abdul Aziz, Z.A., Nasir, H.M., Ahmad, A., Setapar, S.H., Ahmad, H., Noor, M.H., Rafatullah, M., Khatoon, A., Kausar, M.A., Ahmad, I., Khan, S., Al-Shaeri, M., Ashraf, G.M., 2019. Enrichment of eucalyptus oil nanoemulsion by micellar nanotechnology: Transdermal analgesic activity using hot plate test in rats' assay. Sci. Rep. 9, 1–16. https://doi.org/10.1038/s41598-019-50134-y.

Abdul Rasool, B.K., Mohammed, A.A., Salem, Y.Y., 2021. The optimization of a dimenhydrinate transdermal patch formulation based on the quantitative analysis of in vitro release data by DDSolver through skin penetration studies. Sci. Pharm. 89, 33. https://doi.org/10.3390/scipharm89030033.

Aderibigbe, B., 2018. In situ-based gels for nose to brain delivery for the treatment of neurological diseases. Pharmaceutics 10, 40. https://doi.org/10.3390/pharmaceutics10020040.

Adnet, T., Groo, A., Picard, C., Davis, A., Corvaisier, S., Since, M., Bounoure, F., Rochais, C., Le Pluart, L., Dallemagne, P., Malzert-Fréon, A., 2020. Pharmacotechnical development of a nasal drug delivery composite nanosystem intended for Alzheimer's disease treatment. Pharmaceutics 12, 251. https://doi.org/10.3390/pharmaceutics12030251.

Aggarwal, N., Goindi, S., Khurana, R., 2013. Formulation, characterization and evaluation of an optimized microemulsion formulation of griseofulvin for topical application. Colloids Surf. B: Biointerfaces 105, 158–166. https://doi.org/10.1016/j.colsurfb.2013.01.004.

Aiswarya, G., Reza, K., Rajan, R., 2015. Development, evaluation, and optimization of flurbiprofen nanoemulsions gel using quality by design concept. Asian J. Pharm. 9, 35–43. https://doi.org/10.4103/0973-8398.150035.

Akhtar, J., Siddiqui, H.H., Fareed, S., Badruddeen, Khalid, M., Aqil, M., 2016. Nanoemulsion: For improved oral delivery of repaglinide. Drug Deliv. 23 (6), 2026–2034. https://doi.org/10.3109/10717544.2015.1077290.

Al Khateb, K., Ozhmukhametova, E.K., Mussin, M.N., Seilkhanov, S.K., Rakhypbekov, T.K., Lau, W.M., Khutoryanskiy, V.V., 2016. In situ gelling systems based on Pluronic F127/Pluronic F68 formulations for ocular drug delivery. Int. J. Pharm. 502 (1-2), 70–79. https://doi.org/10.1016/j.ijpharm.2016.02.027.

Alanazi, F.K., Haq, N., Radwan, A.A., Alsarra, I.A., Shakeel, F., 2013. Formulation and evaluation of cholesterol-rich nanoemulsion (LDE) for drug delivery potential of cholesteryl-maleoyl-5-fluorouracil. Pharm. Dev. Tech. 20 (3), 266–270. https://doi.org/10.3109/10837450.2013.860551.

Altuntaş, E., Yener, G., 2017. Formulation and evaluation of thermoreversible in situ nasal gels containing mometasone furoate for allergic rhinitis. AAPS PharmSciTech. 18 (7), 2673–2682. https://doi.org/10.1208/s12249-017-0747-8.

Anderson, B.C., Pandit, N.K., Mallapragada, S.K., 2001. Understanding drug release from poly(ethylene oxide)-B-poly(propylene oxide)-B-poly(ethylene oxide) gels. J. Control. Release 70 (1-2), 157–167. https://doi.org/10.1016/S0168-3659(00)00341-2.

Arora, R., Aggarwal, G., Harikumar, S.L., Kaur, K., 2014. Nanoemulsion based hydrogel for enhanced transdermal delivery of ketoprofen. Adv. Pharm. 2014, 1–12. https://doi.org/10.1155/2014/468456.

Atodaria, E., Mashru, R., 2018. Development and validation of some classical and novel spectrophotometric methods and RP-HPLC method by QbD approach for simultaneous estimation of aripiprazole and clozapine in synthetic mixture. World J. Pharm. Res. 7, 521–557.

Azeem, A., Rizwan, M., Ahmad, F.J., Iqbal, Z., Khar, R.K., Aqil, M., Talegaonkar, S., 2009. Nanoemulsion components screening and selection: a technical note. AAPS PharmSciTech. 10 (1), 69–76. https://doi.org/10.1208/s12249-008-9178-x.

Baboota, S., Shakeel, F., Ahuja, A., Ali, J., Shafiq, S., 2007. Design, development and evaluation of novel nanoemulsion formulations for transdermal potential of celecoxib. Acta Pharm. 57, 315–332. https://doi.org/10.2478/v10007-007-0025-5.

Baghel, P., Roy, A., Verma, S., Satapathy, T., Bahadur, S., 2020. Amelioration of lipophilic compounds in regards to bioavailability as self-emulsifying drug delivery system (SEDDS). Future J. Pharm. Sci. 6, 21. https://doi.org/10.1186/s43094-020-00042-0.

Balata, G.F., Essa, E.A., Shamardl, H.A., Zaidan, S.H., Abourehab, M.A.S., 2016. Self-emulsifying drug delivery systems as a tool to improve solubility and bioavailability of resveratrol. Drug Des. Dev. Ther. 10, 117–128. https://doi.org/10.2147/DDDT.S95905.

Basu, S., Bandyopadhyay, A.K., 2010. Development and characterization of mucoadhesive in situ nasal gel of midazolam prepared with ficus carica mucilage. AAPS PharmSciTech. 11 (3), 1223–1231. https://doi.org/10.1208/s12249-010-9477-x.

Bayanati, M., Khosroshahi, A.G., Alvandi, M., Mahboobian, M.M., Sun, F., 2021. Fabrication of a thermosensitive in situ gel nanoemulsion for nose to brain delivery of temozolomide. J. Nanomater. 2021, 1–11. https://doi.org/10.1155/2021/1546798.

Bhattacharjee, k., 2019. Importance of surface energy in nanoemulsion, in: Koh, K.S., Wong, V.L. (Eds.), Nanoemulsions - Properties, Fabrications and Applications, IntechOpen, Croatia, pp. 87–106.

Bonacucina, G., Cespi, M., Mencarelli, G., Giorgioni, G., Palmieri, G.F., 2011. Thermosensitive self-assembling block copolymers as drug delivery systems. Polymers 3, 779–811. https://doi.org/10.3390/polym3020779.

Bonferoni, M.C., Rossi, S., Sandri, G., Ferrari, F., Gavini, E., Rassu, G., Giunchedi, P., 2019. Nanoemulsions for ''nose-to-brain'' drug delivery. Pharmaceutics 11, 84. https://doi.org/10.3390/pharmaceutics11020084.

Chaudhari, B., Saldanha, D., Kadiani, A., Shahani, R., 2017. Evaluation of treatment adherence in outpatients with schizophrenia. Ind. Psychiatry J. 26, 215–222. https://doi.org/10.4103/ipj.ipj_24_17.

Chaudhary, B., Verma, S., 2014. Preparation and evaluation of novel in situ gels containing acyclovir for the treatment of oral herpes simplex virus infections. Sci. World J. 2014, 1–7. https://doi.org/10.1155/2014/280928.

Chen, E., Chen, J., Cao, S.-lei., Zhang, Q.-zhi., Jiang, X.-guo., 2010. Preparation of nasal temperature-sensitive in situ gel ofRadix Bupleuriand evaluation of the febrile response mechanism. Drug Dev. Ind. Pharm. 36 (4), 490–496. https://doi.org/10.3109/03639040903264371.

Chime, S.A., Kenechukwu, F.C., Attama, A.A., 2014. Nanoemulsions–Advances in formulation, characterization and applications in drug delivery, in: Sezer, A.D. (Ed.), Application of Nanotechnology in Drug Delivery. IntechOpen, Croatia, pp. 77–126.

Chintalapudi, R., Murthy, T.E., Lakshmi, K., Manohar, G., 2015. Formulation, optimization, and evaluation of self-emulsifying drug delivery systems of nevirapine. Int. J. Pharm. Investig. 5, 205–213. https://doi.org/10.4103/2230-973x.167676.

Craciun, A., Barhalescu, M.L., Agop, M., Ochiuz, L., 2019. Theoretical modeling of long-time drug release from nitrosalicyl-imine-Chitosan hydrogels through multifractal logistic type laws. Comput. Math. Methods Med. 2019, 1–10. https://doi.org/10.1155/2019/4091464.

Edresi, S., Baie, S., 2009. Formulation and stability of whitening VCO-in-water nanocream. Int. J. Pharm. 373 (1-2), 174–178. https://doi.org/10.1016/j.ijpharm.2009.02.011.

Edris, A.E., Abd El-Galeel, M.A.S., 2010. Solubilization of some flavor and fragrance oils in surfactant/water system. World Appl. Sci. J. 8, 86–91.

Elbardisy, B., Galal, S., Abdelmonsif, D.A., Boraie, N., 2019. Intranasal Tadalafil nanoemulsions: Formulation, characterization and pharmacodynamic evaluation. Pharm. Dev. Technol. 24 (9), 1083–1094. https://doi.org/10.1080/10837450.2019.1631846.

Elshafeey, A.H., Bendas, E.R., Mohamed, O.H., 2009. Intranasal microemulsion of sildenafil citrate: in vitro evaluation and in vivo pharmacokinetic study in rabbits. AAPS PharmSciTech. 10 (2), 361–367. https://doi.org/10.1208/s12249-009-9213-6.

Escobar-Chávez, J.J., López-Cervantes, M., Naïk, A., Kalia, Y.N., Quintanar-Guerrero, D., Ganem-Quintanar, A., 2006. Applications of thermoreversible pluronic F-127 gels in pharmaceutical formulations. J. Pharm. Pharmaceut. Sci. 9, 339–358.

Fakhar-Ud-Din, Khan, G.M., 2017. Development and characterisation of levosulpiride-loaded suppositories with improved bioavailability in vivo. Pharm. Dev. Technol. 24, 63–69. https://doi.org/10.1080/10837450.2017.1419256.

Fakhari, A., Corcoran, M., Schwarz, A., 2017. Thermogelling properties of purified poloxamer 407. Heliyon 3 (8), e00390. https://doi.org/10.1016/j.heliyon.2017.e00390.

Food and Drug Adminstration (FDA), 2021. Information on Clozapine. https://www.fda.gov/drugs/postmarket-drug-safety-information-patients-and-providers/information-clozapine (accessed 20 September 2021).

Furubayashi, T., Inoue, D., Kamaguchi, A., Higashi, Y., Sakane, T., 2007. Influence of formulation viscosity on drug absorption following nasal application in rats. Drug Metab. Pharmacokinet. 22 (3), 206–211. https://doi.org/10.2133/dmpk.22.206.

Gaba, B., Khan, T., Haider, M.F., Alam, T., Baboota, S., Parvez, S., Ali, J., 2019. Vitamin E loaded naringenin nanoemulsion via intranasal delivery for the management of oxidative stress in a 6-OHDA Parkinson's disease model. Biomed Res. Int. 2019, 1–20. https://doi.org/10.1155/2019/2382563.

Grinchii, D., Dremencov, E., 2020. Mechanism of action of atypical antipsychotic drugs in mood disorders. Int. J. Mol. Sci. 21, 9532. https://doi.org/10.3390/ijms21249532.

Hashemnejad, S.M., Badruddoza, A.Z., Zarket, B., Ricardo Castaneda, C., Doyle, P.S., 2019. Thermoresponsive nanoemulsion-based gel synthesized through a low-energy process. Nat. Commun. 10, 1–10. https://doi.org/10.1038/s41467-019-10749-1.

He, W., Tan, Y., Tian, Z., Chen, L., Hu, F., Wu, W., 2011. Food protein-stabilized nanoemulsions as potential delivery systems for poorly water-soluble drugs: preparation, in vitro characterization, and pharmacokinetics in rats. Int. J. Nanomed. 6, 521–533. https://doi.org/10.2147/IJN.S17282.

Hosny, K.M., Rizg, W.Y., Khallaf, R.A., 2020. Preparation and optimization of in situ gel loaded with rosuvastatin-ellagic acid nanotransfersomes to enhance the anti-proliferative activity. Pharmaceutics 12, 263. https://doi.org/10.3390/pharmaceutics12030263.

Huo, P., Han, X., Zhang, W., Zhang, J., Kumar, P., Liu, B., 2021. Electrospun nanofibers of polycaprolactone/collagen as a sustained-release drug delivery system for artemisinin. Pharmaceutics 13, 1228. https://doi.org/10.3390/pharmaceutics13081228.

Ibrahim, T.M., Abdallah, M.H., El-Megrab, N.A., El-Nahas, H.M., 2018. Upgrading of dissolution and anti-hypertensive effect of Carvedilol via two combined approaches: Self-emulsification and liquisolid techniques. Drug Dev. Ind. Pharm. 44 (6), 873–885. https://doi.org/10.1080/03639045.2017.1417421.

Ibrahim, T.M., El-Megrab, N.A., El-Nahas, H.M., 2021. An overview of PLGA in-situ forming implants based on solvent exchange technique: Effect of formulation components and characterization. Pharm. Dev. Technol. 26 (7), 709–728. https://doi.org/10.1080/10837450.2021.1944207.

Idrees, M., Rahman, N., Ahmad, S., Ali, M., Ahmad, I., 2011. Enhance transdermal delivery of flurbiprofen via microemulsions: Effects of different types of surfactants and cosurfactants. DARU J. Pharm. Sci. 19, 433–439.

Jagdale, S., Shewale, N., Kuchekar, B.S., 2016. Optimization of thermoreversible in situ nasal gel of timolol maleate. Scientifica 2016, 1–11. https://doi.org/10.1155/2016/6401267.

Jaiswal, J., Anantvar, S.P., Narkhede, M.R., Gore, S.V., Mehta, K., 2012. Formulation and evaluation of thermoreversible insitu nasal gel of metoprolol succinate. Int. J. Pharm. Pharm. Sci. 4, 96–102. https://doi.org/10.22159/ijcpr.2017v9i5.22135.

Jeevanandam, J., Barhoum, A., Chan, Y.S., Dufresne, A., Danquah, M.K., 2018. Review on nanoparticles and nanostructured materials: History, sources, toxicity and regulations. Beilstein J. Nanotechnol. 9, 1050–1074. https://doi.org/10.3762/bjnano.9.98.

John, M.S., Nair, S.C., Anoop, K.P., 2013. Thermoreversible mucoadhesive gel for nasal delivery of anti-hypertensive drug. Int. J. Pharm. Sci. Rev. Res. 21, 57–63.

Juniatik, M., Hidayati, K., Wulandari, F.P., Pangestuti, N., Munawaroh, N., Martien, R., Utami, S., 2017. Formulation of nanoemulsion mouthwash combination of lemongrass oil (cymbopogon citratus) and kaffir lime oil (citrus hystrix) against candida albicans ATCC 10231. Trad. Med. J. 22, 7–15. https://doi.org/10.22146/tradmedj.24255.

Khani, S., Keyhanfar, F., Amani, A., 2015. Design and evaluation of oral nanoemulsion drug delivery system of mebudipine. Drug Deliv. 23 (6), 2035–2043. https://doi.org/10.3109/10717544.2015.1088597.

Kolsure, P.K., Rajkapoor, B., 2012. Development of zolmitriptan gel for nasal administration. Asian J. Pharm. Clin. Res. 5, 88–94.

Kourniatis, L.R., Spinelli, L.S., Piombini, C.R., Mansur, C.R.E., 2010. Formation of orange oil-in-water nanoemullsions using nonionic surfactant mixtures by high pressure homogenizer. Colloid J. 72 (3), 396–402. https://doi.org/10.1134/S1061933X10030130.

Kreilgaard, M., Pedersen, E.J., Jaroszewski, J.W., 2000. NMR characterization and transdermal drug delivery potential of microemulsion systems. J. Control. Release 69, 421–433. https://doi.org/10.1016/S0168-3659(00)00325-4.

Mahaparale, S.P., Gaware, V., 2017. Formulation and evaluation of lornoxicam emulgel. Int. J. Pharm. Chem. Anal. 4, 83–87. https://doi.org/10.18231/2394-2797.2017.0019.

Mahdi, E.S., Sattar, M., Sakeena, M., Abdulkarim, M., Noor, A.M., Abdullah, G., 2011. Effect of surfactant and surfactant blends on pseudoternary phase diagram behavior of newly synthesized palm kernel oil esters. Drug Des. Devel. Ther. 5, 311–323. https://doi.org/10.2147/dddt.s15698.

Maheswara, R.C., Firoz, S., Rajalakshmi, R., Ashok, K.C.K., 2011. Design and evaluation of chloramphenicol thermoreversible in situ gels for ocular drug delivery. Int. J. Innov. Pharm. Res. 2, 131–138.

Manjunath, K., Venkateswarlu, V., 2005. Pharmacokinetics, tissue distribution and bioavailability of clozapine solid lipid nanoparticles after intravenous and intraduodenal administration. J. Control. Release 107 (2), 215–228. https://doi.org/10.1016/j.jconrel.2005.06.006.

Martindale, W., 2014. The complete drug reference. Pharmaceutical Press, London.

Mbah, C.C., Builders, P.F., Agubata, C.O., Attama, A.A., 2019. Development of ethosomal vesicular carrier for topical application of griseofulvin: effect of ethanol concentration. Int. J. Pharm. Investig. 49 (1), 27–36. https://doi.org/10.1007/s40005-017-0367-z.

Mohamad, S.A., Safwat, M.A., Elrehany, M., Maher, S.A., Badawi, A.M., Mansour, H.F., 2021. A novel nasal co-loaded loratadine and sulpiride nanoemulsion with improved downregulation of TNF-α, TGF-β and IL-1 in rabbit models of ovalbumin-induced allergic rhinitis. Drug Deliv. 28 (1), 229–239. https://doi.org/10.1080/10717544.2021.1872741.

Moradi, S., Barati, A., 2019. Essential oils nanoemulsions: Preparation, characterization and study of antibacterial activity against escherichia coli. Int. J. Nanosci. Nanotechnol. 15, 199–210.

Morsy, M.A., Abdel-Latif, R.G., Nair, A.B., Venugopala, K.N., Ahmed, A.F., Elsewedy, H. S., Shehata, T.M., 2019. Preparation and evaluation of atorvastatin-loaded Nanoemulgel on wound-healing efficacy. Pharmaceutics 11, 609. https://doi.org/10.3390/pharmaceutics11110609.

Mura, P., Bragagni, M., Mennini, N., Cirri, M., Maestrelli, F., 2014. Development of liposomal and microemulsion formulations for transdermal delivery of clonazepam: Effect of randomly methylated β-cyclodextrin. Int. J. Pharm. 475 (1-2), 306–314. https://doi.org/10.1016/j.ijpharm.2014.08.066.

Mura, S., Manconi, M., Valenti, D., Sinico, C., Vila, A.O., Fadda, A.M., 2011. Transcutol containing vesicles for topical delivery of minoxidil. J. Drug Target. 19 (3), 189–196. https://doi.org/10.3109/1061186X.2010.483516.

Naeem, M., Rahman, N.U., Tavares, G.D., Barbosa, S.F., Chacra, N.B., Löbenberg, R., Sarfraz, M.K., 2015. Physicochemical, in vitro and in vivo evaluation of flurbiprofen microemulsion. An. Acad. Bras. Ciênc. 87, 1823–1831. https://doi.org/10.1590/0001-3765201520130436.

Novakovic, V., Sher, L., 2012. The use of clozapine for the treatment of schizophrenia and implications for suicide prevention. Int. J. Disabil. Hum. Dev. 11, 5–8. https://doi.org/10.1515/ijdhd.2012.010.

Okur, N.U., Yozgatli, V., Senyigit, Z., 2020. Formulation and detailed characterization of voriconazole loaded in situ gels for ocular application. J. Fac. Pharm. Ankara 44, 33–49. https://doi.org/10.33483/jfpau.586590.

Omar, M.M., Eleraky, N.E., El Sisi, A.M., Hasan, O.A., 2019. Development and evaluation of in-situ nasal gel formulations of nanosized transferosomal sumatriptan: Design, optimization, in vitro and in vivo evaluation. Drug Des. Devel. Ther. 13, 4413–4430. https://doi.org/10.2147/DDDT.S235004.

Opare-Addo, M.N., Mensah, J., Aboagye, G.O., 2020. A case of schizophrenia in a young male adult with no history of substance abuse: Impact of clinical pharmacists' interventions on patient outcome. Case Rep. Psychiatry 2020, 1–5. https://doi.org/10.1155/2020/3419609.

Panda, A., Meena, J., Katara, R., Majumdar, D.K., 2016. Formulation and characterization of clozapine and risperidone co-entrapped spray-dried PLGA nanoparticles. Pharm. Dev. Technol. 21 (1), 43–53. https://doi.org/10.3109/10837450.2014.965324.

Patel, H.P., Chaudhari, P.S., Gandhi, P.A., Desai, B.V., Desai, D.T., Dedhiya, P.P., Vyas, B. A., Maulvi, F.A., 2021a. Nose to brain delivery of tailored clozapine nanosuspension stabilized using (+)-Alpha-tocopherol polyethylene glycol 1000 succinate: Optimization and in vivo pharmacokinetic studies. Int. J. Pharm. 600, 120474. https://doi.org/10.1016/j.ijpharm.2021.120474.

Patel, H.P., Gandhi, P.A., Chaudhari, P.S., Desai, B.V., Desai, D.T., Dedhiya, P.P., Maulvi, F.A., Vyas, B.A., 2021b. Clozapine loaded nanostructured lipid carriers engineered for brain targeting via nose-to-brain delivery: Optimization and in vivo pharmacokinetic studies. J. Drug Deliv. Sci. Technol. 64, 102533. https://doi.org/10.1016/j.jddst.2021.102533.

Patel, K.R., Cherian, J., Gohil, K., Atkinson, D., 2014. Schizophrenia: overview and treatment options. Pharm. Therap. 39, 638–645.

Patel, M.R., Patel, M.H., Patel, R.B., 2016. Preparation and in vitro/ex vivo evaluation of nanoemulsion for transnasal delivery of paliperidone. Appl. Nanosci. 6 (8), 1095–1104. https://doi.org/10.1007/s13204-016-0527-x.

Pavoni, L., Perinelli, D.R., Bonacucina, G., Cespi, M., Palmieri, G.F., 2020. An overview of micro- and nanoemulsions as vehicles for essential oils: Formulation, preparation and stability. Nanomaterials 10, 135. https://doi.org/10.3390/nano10010135.

Prabhakar, K., Afzal, S.M., Surender, G., Kishan, V., 2013. Tween 80 containing lipid nanoemulsions for delivery of indinavir to brain. Acta Pharm. Sin. B. 3 (5), 345–353. https://doi.org/10.1016/j.apsb:2013.08.001.

Qian, S., Wong, Y.C., Zuo, Z., 2014. Development, characterization and application of in situ gel systems for intranasal delivery of tacrine. Int. J. Pharm. 468 (1-2), 272–282. https://doi.org/10.1016/j.ijpharm.2014.04.015.

Roohinejad, S., Oey, I., Wen, J., Lee, S.J., Everett, D.W., Burritt, D.J., 2015. Formulation of oil-in-water β-carotene microemulsions: Effect of oil type and fatty acid chain length. Food Chem. 174, 270–278. https://doi.org/10.1016/j.foodchem.2014.11.056.

Russo, E., Villa, C., 2019. Poloxamer hydrogels for biomedical applications. Pharmaceutics 11 (12), 671. https://doi.org/10.3390/pharmaceutics11120671.

Sankar, V., Ruckmani, K., Durga, S., Jailani, S., 2010. Proniosomes as drug carriers. Pak. J. Pharm. Sci. 23, 103–107.

Sarwal, A., Singh, G., Singh, S., Singh, K., Sinha, V.R., 2019. Novel and effectual delivery of an antifungal agent for the treatment of persistent vulvovaginal candidiasis. J. Pharm. Investig. 49 (1), 135–147. https://doi.org/10.1007/s40005-018-0395-3.

Sayed, S., Elsharkawy, F.M., Amin, M.M., Shamsel-Din, H.A., Ibrahim, A.B., 2021. Brain targeting efficiency of intranasal clozapine-loaded mixed micelles following radio labeling with technetium-99m. Drug Deliv. 28 (1), 1524–1538. https://doi.org/10.1080/10717544.2021.1951895.

Schreiner, T.B., Santamaria-Echart, A., Ribeiro, A., Peres, A.M., Dias, M.M., Pinho, S.P., Barreiro, M.F., 2020. Formulation and optimization of nanoemulsions using the natural surfactant saponin from quillaja bark. Molecules 25, 1538. https://doi.org/10.3390/molecules25071538.

Shafiq, S., Shakeel, F., Talegaonkar, S., Ahmad, F.J., Khar, R.K., Ali, M., 2007. Development and bioavailability assessment of ramipril nanoemulsion formulation. Eur. J. Pharm. Biopharm. 66 (2), 227–243. https://doi.org/10.1016/j.ejpb.2006.10.014.

Shah, J., Nair, A.B., Jacob, S., Patel, R.K., Shah, H., Shehata, T.M., Morsy, M.A., 2019. Nanoemulsion based vehicle for effective ocular delivery of moxifloxacin using experimental design and pharmacokinetic study in rabbits. Pharmaceutics 11, 230. https://doi.org/10.3390/pharmaceutics11050230.

Sheth, T., Seshadri, S., Prileszky, T., Helgeson, M.E., 2020. Multiple nanoemulsions. Nat. Rev. Mater. 5 (3), 214–228. https://doi.org/10.1038/s41578-019-0161-9.

Sita, V.G., Vavia, P., 2020. Bromocriptine nanoemulsion-loaded transdermal gel: Optimization using factorial design, in vitro and in vivo evaluation. AAPS PharmSciTech. 21, 80. https://doi.org/10.1208/s12249-020-1620-8.

Song, Y., Wang, X., Wang, X., Wang, J., Hao, Q., Hao, J., Hou, X., Morroni, F., 2021. Osthole-loaded Nanoemulsion enhances brain target in the treatment of Alzheimer's disease via intranasal administration. Oxid. Med. Cell. Longev. 2021, 1–16. https://doi.org/10.1155/2021/8844455.

Stępnicki, P., Kondej, M., Kaczor, A.A., 2018. Current concepts and treatments of schizophrenia. Molecules 23, 2087. https://doi.org/10.3390/molecules23082087.

Sulaimon, A.A., Adeyemi, B.J., 2018. Effects of interfacial tension alteration on the destabilization of water-oil emulsions, in: Karakus S. (Ed.), Science and Technology Behind Nanoemulsions, IntechOpen, Croatia, pp. 83–110.

Syed, H.K., Peh, K.K., 2014. Identification of phases of various oil, surfactant/co-surfactants and water system by ternary phase diagram. Acta Pol. Pharm. 71, 301–309.

Tan, M.S., Parekh, H.S., Pandey, P., Siskind, D.J., Falconer, J.R., 2020. Development and optimization of clozapine-loaded PLGA nanoparticles for nose-to-brain delivery using supercritical fluid. PSWC, 2020 Virtual.

Tareen, F.K., Shah, K.U., Ahmad, N., Rehman, A., Shah, S.U., Ullah, N., 2020. Proniosomes as a carrier system for transdermal delivery of clozapine. Drug Dev. Ind. Pharm. 46, 946–954. https://doi.org/10.1080/03639045.2020.176402.

Tung, N.-T., Tran, C.-S., Pham, T.-M.-H., Nguyen, H.-A., Nguyen, T.-L., Chi, S.-C., Nguyen, D.-D., Bui, T.-B.-H., 2018. Development of solidified self-microemulsifying drug delivery systems containing l-tetrahydropalmatine: Design of experiment approach and bioavailability comparison. Int. J. Pharm. 537 (1-2), 9–21. https://doi.org/10.1016/j.ijpharm.2017.12.027.

Velupula, R., Janapareddi, K., 2019. Development and evaluation of clozapine intranasal mucoadhesive in situ gels for brain targeting. J. Drug Deliv. Ther. 9, 198–207. https://doi.org/10.22270/jddt.v9i2-s.2491.

Venkateswarlu, V., Manjunath, K., 2004. Preparation, characterization and in vitro release kinetics of clozapine solid lipid nanoparticles. J. Control. Release 95 (3), 627–638. https://doi.org/10.1016/j.jconrel.2004.01.005.

Vibha, B., 2014. In-situ gel nasal drug delivery system-a review. Int. J. Pharma Sci. 4, 577–580.

Wang, X., Liu, G., Ma, J., Guo, S., Gao, L., Jia, Y., Li, X., Zhang, Q., 2013. In situ gel-forming system: An attractive alternative for nasal drug delivery. Crit. Rev. Ther. Drug Carrier Syst. 30 (5), 411–434. https://doi.org/10.1615/CritRevTherDrugCarrierSyst.2013007362.

Wang, Y., Jiang, S., Wang, H., Bie, H., Xu, B., 2017. A mucoadhesive, thermoreversible in situ nasal gel of geniposide for neurodegenerative diseases. PLOS ONE 12 (12), e0189478.

Wong, P.T., Wang, S.H., Ciotti, S., Makidon, P.E., Smith, D.M., Fan, Y., Schuler, C.F., Baker, J.R., 2013. Formulation and characterization of nanoemulsion intranasal adjuvants: Effects of surfactant composition on mucoadhesion and immunogenicity. Mol. Pharm. 11 (2), 531–544. https://doi.org/10.1021/mp4005029.

Zaki, N.M., Awad, G.A., Mortada, N.D., Abd ElHady, S.S., 2007. Enhanced bioavailability of metoclopramide HCl by intranasal administration of a mucoadhesive in situ gel with modulated rheological and mucociliary transport properties. Eur. J. Pharm. Sci. 32 (4-5), 296–307. https://doi.org/10.1016/j.ejps.2007.08.006.

Zhao, L., Wang, Y., Zhai, Y., Wang, Z., Liu, J., Zhai, G., 2014. Ropivacaine loaded microemulsion and microemulsion-based gel for transdermal delivery: preparation, optimization, and evaluation. Int. J. Pharm. 477 (1-2), 47–56. https://doi.org/10.1016/j.ijpharm.2014.10.005.